A review of metallic materials for latent heat thermal energy storage: thermophysical properties, applications, and challenges

Sol Carolina Costa[1,*] and Murat Kenisarin

[1]Department of Mechanical and Construction Engineering, Northumbria University, Wynne-Jones Centre, Newcastle upon Tyne NE1 8ST, UK

*Corresponding author: carolina.costa@northumbria.ac.uk, +44 (0) 191 243 7649

Abstract

Phase change materials provide desirable characteristics for latent heat thermal energy storage by keeping the high energy density and quasi isothermal working temperature. Along with this, the most promising phase change materials, including organics and inorganic salt hydrate, have low thermal conductivity as one of the main drawbacks. Metallic materials are attractive alternatives due to their higher thermal conductivity and high volumetric heat storage capacity. This paper presents an extensive review of the thermophysical properties of metals and alloys as the potential phase change materials for low (< 40°C), medium (40°C - 300°C), and high (> 300°C) temperatures. The information presented includes the fundamental thermophysical properties as melting temperature, the heat of fusion, density, specific heat, and thermal conductivity found in the published literature. The temperature dependence of critical properties as specific heat, density, thermal conductivity, expansion coefficient, viscosity is also reviewed, including mathematical theoretical predictions crucial from an engineering design point of view. Besides, the current work briefly summarises the potential applications and main challenges of metals and alloys as phase change materials. It is intended that this review provides a database of metallic phase change materials thermophysical properties to facilitate the selection, evaluation, and potential impact in different fields as solar energy storage, heating and cooling, electronic, bioengineering, and beyond.

Highlights

- Supercooling and corrosion are the main challenges for low-temperature MPCMs
- Most medium-temperature MPCMs are non-compliant with RoHS directives
- Encapsulation and compatibility are key research topics for LHTES applications
- Simplified design and volume reduction could compensate the MPCMs weight penalties
- Miscibility gap binary alloy, solid-solid and composite are innovative LHTES system

Keywords: Phase change material, metallic, metal alloy, thermal energy storage, latent heat, thermal conductivity.

Word Count: 6300

1. Introduction

Phase change materials (PCMs) provide a useful mode of storing thermal energy as latent heat thermal energy storage (LHTES) due to their high thermal storage density at approximately isothermal conditions. Maria Telkes was pioneered in the study of phase change materials (PCM) for thermal energy storage in the 1940s. However, the interest in this technology appeared during the developing energy crisis of the early 1970s when latent heat storage research and development became a significant part of the solar energy programs [1-6]. In the last years, the interest in PCM has resurfaced considerably, mainly motivated for the deployment of LHTES to bridge the gap between supply and demand in solar energy [7-9]. Recently, the studied range of potential applications for PCM [10, 11] is more extensive, including thermal management in electronic devices and batteries [12-14]; thermal comfort in buildings [15, 16]; domestic space heating, hot water and cooking [17-19]; PV cooling and PV/Thermal[8, 20], vehicle applications [21-23].

At present, many organics and inorganics materials have been investigated as PCMs, those encompassing paraffin, fatty acids, salt hydrates, eutectics compounds, among others. Despite many

years of research in PCMs, selecting an appropriate material for an aimed application is still a challenge, mainly because of the low thermal conductivity, stability, and supercooling of most common organic and salt hydrate PCMs. The low thermal conductivity has an enormous impact on the design of the LHTES system, requiring complicated and costly heat transfer mechanics to charge and discharge the thermal storage [24, 25]. Metallic materials provide relatively high thermal conductivity, high volumetric heat of fusion, and small volume changes, desirable properties to overcome the mentioned issues. In the early '70s, low melting point MPCMs, as Gallium and eutectic alloy 50Bi-26.7Pb-13.3Sn-10Cd (commercially well known as Wood's metal), were studied for thermal control applications in space vehicles [26], and high-temperature eutectic alloys (343 and 947°C) were characterized for solar applications [27-29]. Farkas and Birchenall [29] reported the heat of fusion of eutectics alloys using elements such as Al, Ca, Cu, Mg, P, Si, and Zn. Gasanaliev and Gamataeva [30] characterized metal alloys (between 15.7 to 575°C).

In the high-temperature range, mainly for solar LHTES applications, numerous review papers [21, 31-38] reported the thermodynamic properties obtained by [29, 30] and highlighted their clear advantages of MPCMs in applications for medium and high temperature. In the low-temperature range, few metallic materials are presented in review papers [21] [37, 39-41]. Probably, the review published by Ge et al. [42] is the first dedicated to low melting point metallic PCMs, including about twenty MPCMs with their basic properties in the range of temperature between -38.87 to 271.4°C. There is no consensus on the potential application of metallic materials as PCMs for thermal comfort applications in buildings. Some authors discard the MPCMs due to the high melting point and weight [16, 41, 43], while others pointed out Gallium and some fusible eutectic bismuth-based alloys as possible MPCMs candidates for building applications [44, 45]. The excess weight of MPCMs could be partially offset by the volume reduction and the design simplification of the LHTES due to the high thermal conductivity [21]. In the last years, much of the research efforts in phase change materials have mainly focused on the characterization of thermophysical properties of organic and salt hydrate; for metallic materials, the data found in the literature is incomplete and discrepant [46, 47]. Recently, new promising utilizations of metals and alloys for thermal energy storage has appeared in different research areas: miscibility gap alloys [48-56], metal-organic framework and shape-stabilized PCMs [57-61], encapulation [62-69].The present work aims to provide an extensive and detailed compilation and analysis of the thermophysical properties of metals and alloys as phase change materials. The information presented includes the fundamental thermophysical properties, the temperature dependence of critical properties from the engineering design point of view, a summary of potential applications, and the main challenges of metallic PCMs. It is hoped that this review provides a database of metallic PCMs to facilitate the selection, evaluation, insight into innovative applications, research gaps and new research trends in the area.

Nomenclature

Acronyms/abbreviations

PCM	Phase change material
MPCM	Metallic phase change material
TES	Thermal energy storage
LHTES	Latent heat thermal energy storage
MGA	Miscibility gap binary alloy

Symbols

E_a	Activation Energy (J/mol)
M	Molar mass
R	Gas constant (8.3144 J/mol.K)
T	Temperature (°C)
T_m	Melting temperature (°C)
c_p	Specific heat (J/kg.K)
k	Thermal conductivity (W/m.K)
x	Mole fraction
at.%	Atomic percentage
wt.%	Weight percentage

α	Linear Thermal expansion coefficient (1/K)
β	Volumetric Thermal expansion coeff. (1/K)
ρ	Density (kg/m$^{3)}$
μ	Dynamic viscosity (mPa.s)
ν	Kinematic viscosity (m^2/s)
Subscripts	
i	Element number
m	Melting
s	Solid
l	Liquid

2. Metallic Phase Change Materials (MPCMs)

Metallic PCMs were firstly proposed more than four decades ago [3, 27, 28], and some authors mentioned as potential candidates for different applications [21, 35, 36, 40] highlighting their following advantages:

- Higher thermal conductivity compared to organics and salt hydrates,
- High volumetric heat of fusion,
- Long term stability,
- Relatively low vapor pressure
- Small volume change during melting/freezing.

However, MPCMs have not been systematically studied or evaluated for LHTES applications due to their main drawbacks: weight and cost [16, 33, 37, 39, 42, 70]. The high thermal conductivity is the main advantage of the MPCMs highlighted by many authors [32, 33, 37, 42, 70, 71], and this can simplify enormously the design of thermal energy storage, eliminating the need for heat transfer enhancement techniques.

The classification of PCMs, depending on the melting temperature, in low, medium, or high temperature, depends on the research or applications. In the present review, MPCMs are divided into low-temperature under 40°C, medium-temperature between 40 and 300°C and high-temperature above 300°C. This classification is used in the following section to summarize the MPCMs studies and applications in the last years.

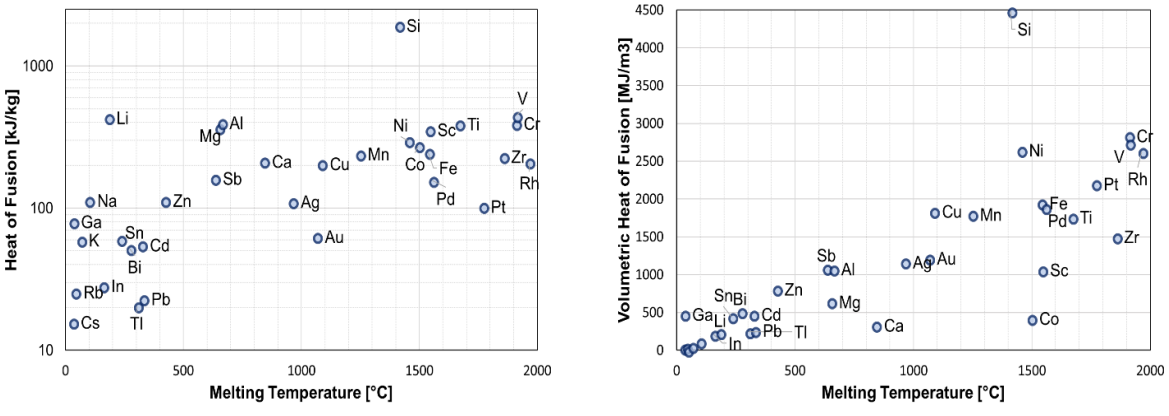

Fig. 1: Specific and Volumetric Latent Heat of some metallic elements

In this section, the authors compile the thermophysical properties and relevant studies published for MPCMs; the metallic PCMs were classified depends on the melting temperature. Figure 1 shows the specific latent heat of fusion and volumetric heat of fusion of pure metallic elements, and Fig. 2 the thermal conductivity and the specific heat. It could be observed that Si is the metallic element with the higher latent heat of fusion and Al with the higher specific heat in the range shown.

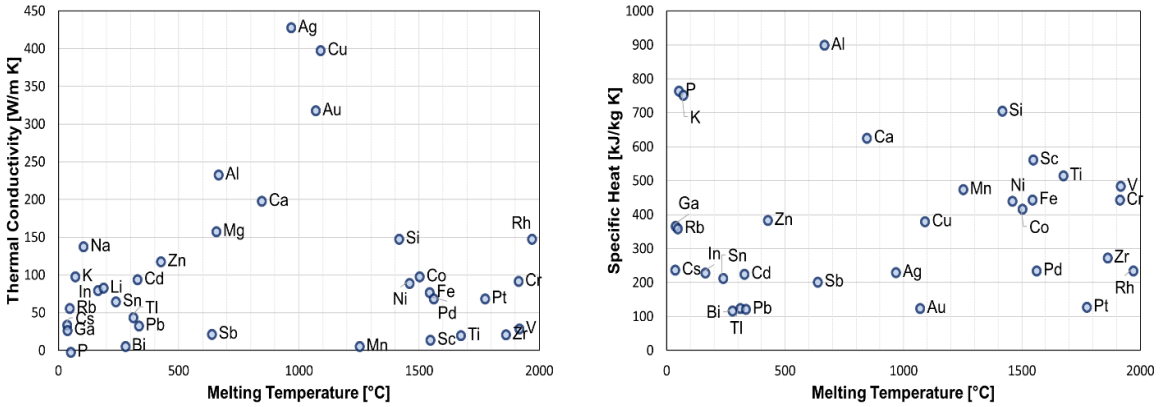

Fig. 2: Thermal Conductivity and Specific Heat of some metallic elements

2.1. High-Temperature MPCMs, Tm > 300°C

Metallic PCMs are good candidates to compete with salts in high-temperature applications because of their high volumetric heat of fusion and excellent thermal reliability [21, 30, 35]. The high-temperature applications are generally associated with concentrated solar power plants, solar energy storage, steam generators, industrial waste-heat recovery. The binary and ternary eutectic alloys of Al, Cu, Mg, Si, and Zn (relatively abundant elements) provide the highest latent heat values, as can be observed in Fig. 1.

In this range of temperature, the most studied alloys were proposed by Birchenall and Riechman [27], mainly the Al-Si alloys [72-76] and Al-Mg-Zn alloys [77] due to their high heat of fusion and relatively low cost [78]. The principal candidate for Al-Si alloys is its eutectic composition, $AlSi_{12}$, it has been studied as a heat storage medium in domestic heaters [72, 79], in steam generators [78, 80-82], in heater for electric and hybrid vehicles [23], in a heat exchanger for industrial heat waste recovery [74], in concentrated solar power plants [83], packed bed LHTES system [84]. In Al-Si alloys, the storage capacity increase with the concentration of Si and the thermal conductivity decrease, as is shown in Fig. 3 [72]. Fig. 4 shows the temperature dependence for specific heat and thermal conductivity obtained by Wang et al. [85] at different cycles.

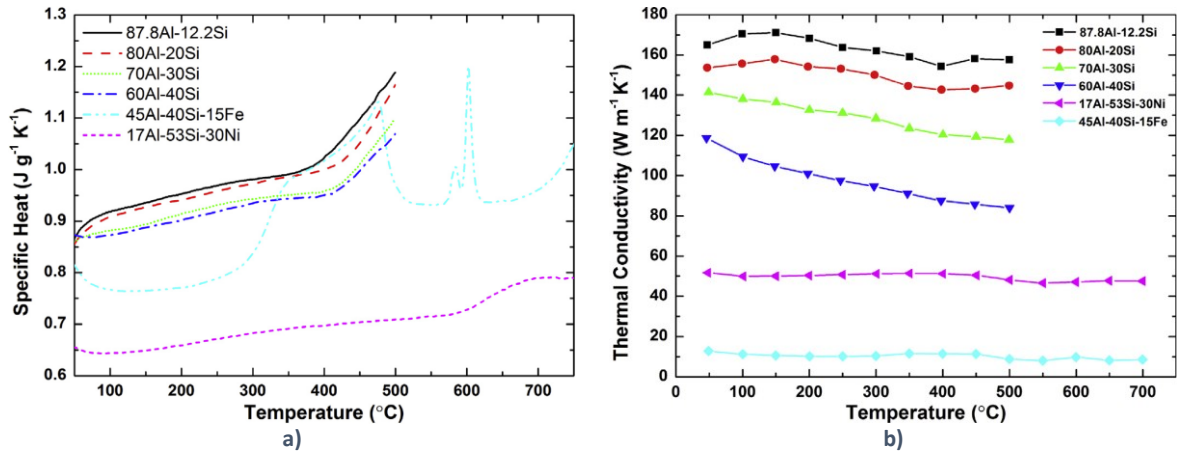

Fig. 3: Properties dependence of temperature for 87.8Al-12.2Si, 80Ale20Si, 70Ale30Si, 60Ale40Si, 45Ale40Sie15Fe, and 17Ale53Sie30Ni: a) Specific Heat measured by DSC and b) Thermal conductivity. Reprinted from [72] with permission from Elsevier.

The compatibility and corrosion problems of Al-Si alloys in high-temperature applications have been studied with graphite-carbon encapsulation material [73], ceramic encapsulation material [64, 86], Al_2O_3 shell encapsulation [87], honeycomb ceramic encapsulation [88], ceramic coated stainless-steel [89], Al_2O_3@Cu multilayer shell [90]. Recently, Li et al. [91] investigated a microstructured metal-based composite that consists of aluminium as PCM and alumina as a skeleton structural supporting material

as a solution for the leakage of corrodible liquid PCMs. Lao et al. [88] results showed a reduction of the latent heat of Al-Si alloys due to the gradual oxidation of Al, losing the storage capacity after the complete transformation of Al to Al_2O_3. Kotze et al. [78, 80-82] pointed out that pure aluminum or eutectic silicon-magnesium alloy were more suitable in practice than $AlSi_{12}$. Sun et al. [77] studied the thermal reliability and corrosion of the Al–34Mg–6Zn (wt.%) and observed that the latent heat of fusion of the alloy decreased 10.98% after 1000 cycles, and the melting temperature changed between 3 to 5K due to the degradation of the chemical structure of the alloy.

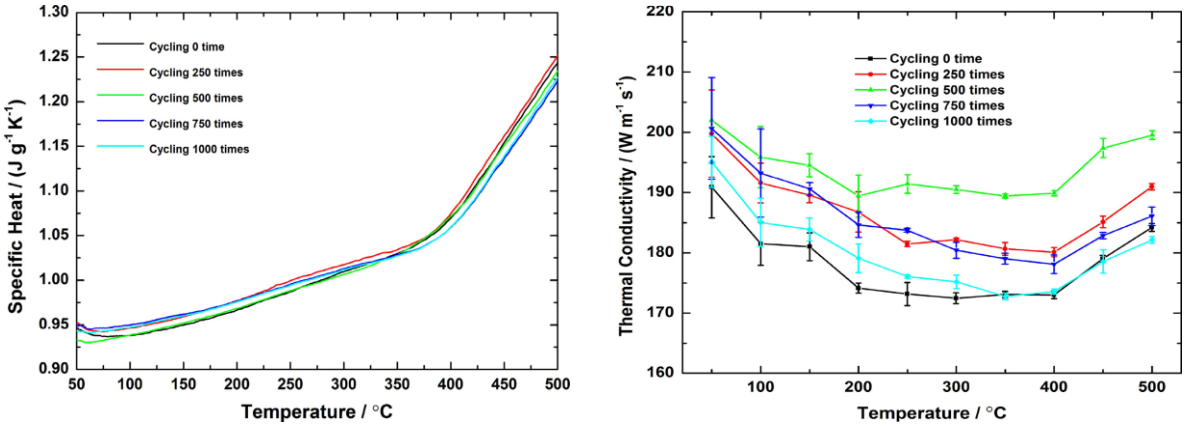

Fig. 4: Properties dependence of temperature for 87.8Al-12.2Si: a) Specific Heat measured by DSC and b) Thermal conductivity calculated. Reprinted from [85] with permission from Elsevier.

The laboratories of CIC Energigune systematically investigated the possibility of using Mg–Zn and Mg–Zn–Al alloys [46, 92-96] for TES in direct steam generation in concentrated solar power applications and for high pressure and high energy steam processes. The selected alloys were Mg-51Zn (wt.%) eutectic [93] and $Mg_{70}Zn_{24.9}Al_{5.1}$ eutectic [95] due to the quasi-constant phase change temperatures (eutectic nature), high heat transfer capacity and better thermal stability [94] [97]. The Zn-rich eutectic alloys, as $Zn_{92.2}Mg_{7.8}$ (at.%), also showed potentiality as MPCMs for their use at CSP plants [47]. Fig. 5a shows the thermal conductivity of the Zn-based alloys, and Fig. 5b is the graphic representation of the specific heat values measured by Risueno et al. [47].

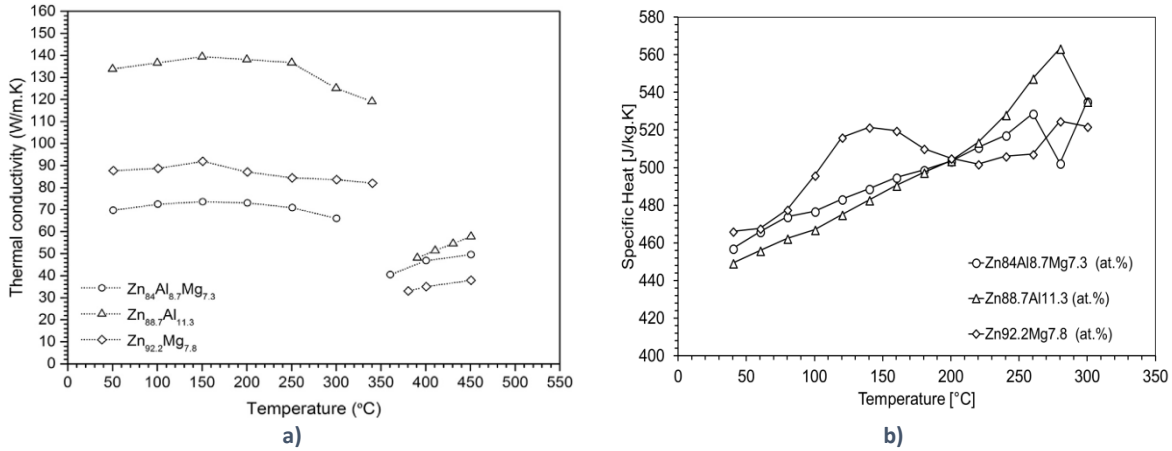

Fig. 5: Properties dependence of temperature for $Zn_{84}Al_{8.7}Mg_{7.3}$, $Zn_{88.7}Al_{11.3}$ and $Zn_{92.2}Mg_{7.8}$ (at.%): a) Thermal conductivity calculated. Reprinted from [47] with permission from Elsevier and b) Graph of Specific Heat measured by [47]

The encapsulation of Cu-based alloys has also been evaluated as a solution to the packaging and corrosion problems. The encapsulation materials include copper capsules coated with refractory metallic shells [62], Fe–shell/Cu-core structure [98], SiC/C-shells/Fe-core capsules [66], graphite-carbon encapsulation material [99].

Fang et al. [100-102] investigated Mg-based alloys as MPCM for TES applications from 400 °C to 600 °C (solar thermal power generation), claiming that its corrosion resistance with encapsulation

materials based on iron is higher than Al-based MPCMs. The measured specific heat and thermal conductivity as a function of the temperature are shown in Fig. 6 for Mg-Bi alloys. The authors found that in Mg-Si alloys, the thermal conductivity decreased with increasing Si content [100]. The thermal expansion increased with rising temperature for Mg-Bi alloys, and the thermal conductivity decreased with increasing Bi content [101]. The same research group [102] recently studied the microstructure and thermal properties of different compositions of Mg-Ni-Zn alloys; as a result, they proposed a ternary alloy Mg-16%Ni-24%Zn as the ideal composition as latent heat storage material.

Xie et al. [76] calculated the thermodynamic data of six Al-based alloys using CALPHAD and compared them with the measured properties using DSC (see Table 1). The results showed that the enthalpy value of Al-4Cu-12Mg-7Si alloy is 85% higher than that of Al-13Si near eutectic alloy, and its initial temperature of phase transformation is about 74°C lower. The authors also pointed out that thermodynamic calculation is valuable in seeking new potential solar energy thermal storage materials for solar thermal power generation systems. Gokon et al. [103] studied the eutectic and hypereutectic compositions of the Fe-Ge alloys as a promised candidate for the next generation of solar thermal applications. Wei et al. [104] proposed an innovative process to prepare Al-Si/Al_2O_3 encapsulated composite PCMs based on the hydrogen generation waste; the process controls the melting temperature of the composite PCMs. Kawaguchi et al. [68] prepared a multilayer microencapsulated Zn-30 Al (wt.%) with the potential to develop new applications at high temperatures.

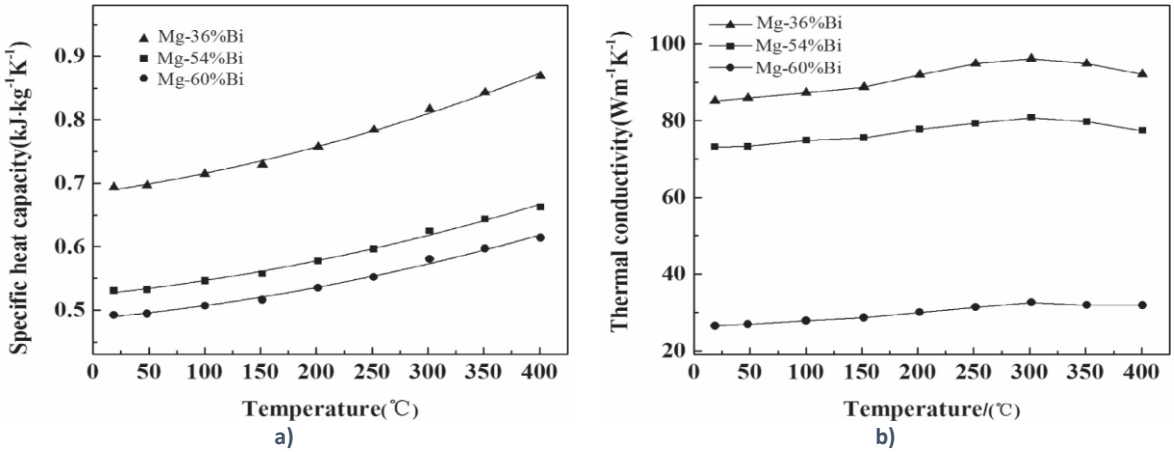

Fig. 6: Properties dependence of temperature for Mg-Bi Alloys: a) Specific Heat measured by DSC and b) Thermal conductivity. Reprinted from [101] with permission from Elsevier.

High-temperature metallic PCMs present serious chemical corrosion issues with the container materials at high-temperature applications, complicating the PCM encapsulation. Encapsulation is the leading approach investigated to alleviate this problem. However, the metallurgical implications, stability under thermal cycling, and manufacturing cost need further evaluation. Recently, Rawson et al.[105] identified the compatible container material for several eutectic metal alloys.

An innovative approach to avoid high-temperature packaging problems is based on using the thermal effect of solid-solid metallic PCMs (Fe-based), which present lower latent heat than solid-liquid transformations (below 60 kJ/kg) [38, 106]. Another solution is the miscibility gap binary alloys (MGA), where one of the alloy components melts (high latent heat) while the other stays solid as a continuous, dense, thermally conductive matrix[50-52]. Sugo et al. [48, 49, 107] proposed an MGA system as high energy-density thermal storage material. They tested two prototypes, Al-Sn and Fe-Cu, claiming that these systems can compete with conventional PCMs due to their high thermal conductivity, high energy density, corrosion resistance, and stability. Recently, Confalonieri et al. [56, 108-110] studied the production methods for MGA based on Al-Sn as phase change material finding the Al-40Sn (wt.%) the most promising alloy. Another newly studied application for metal alloys is their nano-encapsulation to enhance thermal conductivity and thermal storage of conventional PCM as molten salts [111]. Table 1 summarizes the composition, melting temperature, the heat of fusion, density, specific heat, thermal conductivity, and volumetric latent heat for the high temperature (T_m > 300°C) MPCMs being reviewed.

In Table 1, the thermophysical properties are presented with the range of data found in the reference literature. It can be observed that there are significant discrepancies in some of the thermophysical properties reported in the literature, for example, the heat of fusion of eutectic alloys Zn-Al and Al-Si.

Table 1: Main Thermophysical Properties of High-Temperature MPCMs (Melting Point > 300°C)

wt.% Composition (at.%)	T_m (°C)	H_f (kJ/kg)	$\rho_{s/l}$ (kg/m³)	$Cp_{s/l}$ (kJ/kg K)	$k_{s/l}$ (W/m K)	Min $H_{f,v}$ (MJ/m³)	Ref.
Lead (Pb)	327 -328	23 23.8 ± 0.7 23.07 ± 0.14	11340	0.13	35(s) 16.2-17.6 (l)	261	[16, 32, 37, 112-114]
Eutectic Zn-Mg **($MgZn_{28-30}$ at.%)** From 51Zn-49Mg To 53.7Zn-46.3Mg	337 - 343	138 - 210	2850 - 4900	0.71 – 1.04 (s) 1.51(l)	67(s) 55(l) 75 80/50	393	[16, 21, 27, 29, 30, 32, 33, 36, 37, 46, 47, 71, 97, 115, 116]
49Mg-47Zn-4Al **($Mg_{70}Zn_{24.9}Al_{5.1}$ at.%)**	340	132 ± 25 157	2820(s) 2890 - 3000	0.69–0.83(s)	47-59(s) 35 - 38(l)	372	[47, 94, 95, 97, 117, 118]
49.4Mg-46.2Zn-4.4Al **($Mg_{70}Zn_{24.4}Al_{5.6}$ at.%)**	341	157	2730 - 2790	0.70 – 0.72 (s)	41(s) 26(l)	429	[47, 95, 97]
52.2Zn-47.7Mg-0.1Al **($Mg_{71}Zn_{28.9}Al_{0.1}$ at.%)**	343	153	2760 - 3000	0.70(s)	56(s) 27(l)	422	[47, 95, 97]
93.9Zn-3.7Al-2.4Mg **($Zn_{84}Al_{8.7}Mg_{7.3}$ at.%)**	344	132	6546	0.46(s)	71(s) 45(l)	864	[47, 97]
93.86Zn-3.7Al-2.44Mg **($Zn_{85.8}Al_{8.2}Mg_6$ at.%)**	344	104	6190(s)	0.41-0.53(s)	59-55(s) 31(l)	644	[94]
Sn-Zn 70Zn-30Sn	370	107			50(l)		[119]
96.6Zn-3.4Al **($Zn_{92.2}Al_{7.8}$ at.%)**	371	106	6763	0.47(s)	87(s) 34(l)	717	[47, 97]
96Zn-4Al	381	138	6630			915	[21, 30, 32, 33, 36, 37, 71, 75, 116]
Eutectic Zn-Al **($Zn_{88.7}Al_{11.3}$ at.%)** 95Zn-5Al	382	118	6600 - 6752	0.45(s)	122 - 133(s) 48(l)	779	[47, 97, 112, 120]
55Mg-28Ca-17Zn	400	146	2260			330	[29, 71, 116]
46Mg-25Al-15Zn-14Cu	408	205					[121]
Zinc (Zn)	419 - 420	103 - 112	7140 6831(l)	0,39(s) 0,48(l) 0.45	103.1(s)	735	[27, 35, 114, 116, 120, 122, 123]
63.2Mg-32.5Al-4.29Cu	428	282					[117, 118]
59Al-35Mg-6Zn	443	310	2380	1.63 (s) 1.46 (l)		738	[21, 29, 32, 33, 35-37, 71, 75, 116]
60Al-34Mg-6Zn 59.58Al-34Mg-6.42Zn	443 - 450	310 - 329	2380 - 2393	1.05-1.63(s) 1.43-1.46(l)		738	[32, 33, 36, 75, 77, 116]
66Al-34Mg	450	310	2300	1.73(s)	80(s) 50(l)	713	[75]
64.9Al-35.1Mg **($Al_{62.5}Mg_{37.5}$ at.%)**	451	310	2300	1.73	80/50	713	[27, 29]
60Mg-25Cu-15Zn	452	177-254	2800		120-141	711	[21, 29, 32, 33, 35, 36, 71, 116, 124]
60Mg-25Cu-15Ca	453	184	2000			368	[28]
52Mg-25Cu-23Ca	453	184	2000			368	[29, 32, 33, 36, 71, 116]

wt.% Composition (at.%)	T_m (°C)	H_f (kJ/kg)	$\rho_{s/l}$ (kg/m³)	$Cp_{s/l}$ (kJ/kg K)	$k_{s/l}$ (W/m K)	Min $H_{f,v}$ (MJ/m³)	Ref.
45.5Al-24.5Cu-18Zn-12Mg	460-624	315	3800			1197	[75]
48.5Al-26Cu-20.5Zn-5Mg	458-488	164	3860			633	[75]
72Al-15Zn-13Cu	493-598	158	3420			540	[75]
65.35Al-34.65Mg	497	285	2155			614	[30, 32, 33, 36, 37, 71, 116]
60.8Al-33.2Cu-6.0Mg	506	365	3050			1113	[30, 32, 33, 36, 37, 71, 116]
55Al-33Cu-12Mg **($Al_{66.8}Cu_{17}Mg_{16.2}$ at.%)**	506	360	3050	1.09	115/75	1098	[27, 29]
64.6Al-28Cu-5.2Si-2.2Mg	507	374	4400			1646	[21, 30, 32, 33, 36, 71, 75, 116]
54Al-22Cu-18Mg-6Zn	520	305	3140	1.51(s) 1.13(l)		958	[29, 32, 33, 35, 36, 71, 75, 116]
68.5Al-26.5Cu-5Si 67.75Al-27Cu-5.25Si	520 - 525	364 - 366	2938	0.88(s) 1.44(l)		1069	[30, 32, 33, 36, 37, 71, 75, 116]
92.6Al-7.4Cu	528 -646 528-634	339.6-343.5	2860	0.85-1.08(s)	164-199(s)	972	[125]
79Al-21Cu	550-598 526-588	322.9-322.4	3190			1027	[125]
67.9Al-32.1Cu	555-562 535-542	315.9-317.1	3500		149.1(s)	1106	[125]
59.1Al-40.9Cu	546-585 524-570	300.5-296.6	3840			1138	[125]
51.7Cu-48.3Al	589-612 559-585	295.5-286.7	3990		104-114(s)	1143	[125]
64.3Al-34Cu-1.7Sb	545	331	4000			1324	[30, 32, 33, 36, 71, 75, 116]
64Mg-36Bi	548	138	2947 (s)	0.87(s)	92.2(s)	407	[101]
46Mg-54Bi	546	180.5	3094 (s)	0.53(s) 0.66(s)	73(s) 77(s)	558	[101]
60Bi-40Mg	548	48.7	3221 (s)	0.61(s)	31.8(s)	157	[101]
89.65Al-10.35Cu	548-639	285	2889	0.89-0.90(s)	166-180(s)	823	[75]
79.61Al-20.39Cu	552-612	292	3143	0.92-1.09(s)	166-168(s)	917	[75]
69.88Al-30.12Cu	554-569	326	3430	0.65-1.00(s)	123-161(s)	1118	[75]
Eutectic Al-Cu **($Al_{82.5}Cu_{17.5}$ at.%)** From 66.7Al-33.3Cu To 66.92Al-33.08Cu	548	331 - 372	3424 -3600	1.11(s)	130(s) 80(l)	1133	[21, 27, 29, 30, 32, 33, 36, 37, 71, 116, 126]
59.87Al-40.13Cu	559-569	306	3740	0.59-0.51(s)	87-111(s)	1144	[75]
81.8Al-13.2Si-5Mg	552	533		1.12(s) 1.25(l)			[75]
83.14Al-11.7Si-5.16Mg	555	485	2500			1213	[30, 32, 33, 36, 71, 116]
76Mg-24Sn	558	105	2142 ± 25	0.80(s)	58.2(s)	225	[100]
63Mg-37Sn	554	218	2284 ± 18	0.77(s)	52.8(s)	498	[100]
50Mg-50Sn	557	119	2721 ± 49	0.75(s)	32.7(s)	324	[100]
70.6Al-25.5Cu-3.9Mg **($Al_{82.3}Cu_{12.6}Mg_{5.1}$ at.%)**	560	545	2300	1.39	20 70 (l)	1254	[27, 29]
49.1Cu-46.3Al-4.6Si	571	406	5560			2257	[21, 30, 32, 33, 36, 71, 116]

wt.% Composition (at.%)	T_m (°C)	H_f (kJ/kg)	$\rho_{s/l}$ (kg/m³)	$Cp_{s/l}$ (kJ/kg K)	$k_{s/l}$ (W/m K)	Min $H_{f,v}$ (MJ/m³)	Ref.
65Al-30Cu-5Si	571	422	2730	1.30(s) 1.20(l)		1152	[29, 32, 33, 35-37, 71, 75, 116]
86.7Al-10.8Si-2.5Cu (ADC12)	572	441					[86]
75.5Al-23.4Si-1.1Cu (AC9A)	575	395					[86]
86.4Al-9.4Si-4.2Sb	575	471	2700			1272	[30, 32, 33, 36, 71]
92Al-8Si	576	429		1.06(s)			[75]
Eutectic Al-Si **($AlSi_{12-13}$ at.%)** From 88Al-12Si To 86.5Al-13.5Si	557[1] 572 - 580	441 - 519 560[1]	2250 - 2700	0.87 0.94 – 1.49 (s) 1.74(l)	145/158 130/190 160 – 180 (s) 70(l) 75	992	[21, 23, 27, 28, 30, 32, 33, 35-37, 71, 72, 75, 78, 79, 88, 116, 122, 127]
79.4Al-20.6Si 80Al-20Si **($AlSi_{20}$ at.%)**	576 - 585	460 - 553	2580 - 2650	0.97 – 0.98 (s) 1.65(l)	130 158(s)	1187	[21, 32, 33, 36, 37, 72, 75, 79, 88, 116, 127]
80.3Al-19.7Si	587 - 597	372	2634	0.96-1.41(s)	185-220(s)	980	[75]
76.6Al-23.4Si 75Al-25Si	576 - 577	429 - 432	2560	1.04(s) 1.74(l)	167(s) 70(l)	1098	[64, 84, 86]
70Al-30Si **($AlSi_{30}$ at.%)**	580	644	2540	0.90(s)	120-140(s)	1636	[72, 75]
60Al-40Si **($AlSi_{40}$ at.%)**	580	721	2510	0.88(s)	84-110(s)	1810	[72, 75]
Magnesium (Mg)	645 - 651	346 - 377	1590 - 1740	1.27(s) 1.37(l) 1.34	131	550	[27, 35, 48, 116, 122]
79.86Al-10.3Cu-9.84Zn	518-621	267	3110	0.84-0.85(s)	130-135(s)	830	[75]
69.05Al-20.5Cu-10.45Zn	528-583	298	3375	0.64-0.65(s)	88-99(s)	1006	[75]
62.92Al-26.98Cu-10.10Zn	529-543	284	3624	0.64-0.95(s)	99-110(s)	1029	[75]
90.05Al-5.04Zn-4.91Cu	629-647	335	2893	0.87-1.14(s)	155-190(s)	969	[75]
96.48Al-3.52Mg	637-651	290	2660	0.72-0.91(s)	114-155(s)	771	[75]
Aluminium (Al)	660 - 661	388 - 400	2370 - 2700	0,9 (s,l) 1.29	204	920	[16, 32, 35-37, 86, 116, 122]
49Zn-45Cu-6Mg	703 - 705	176	8670	0.42 (s)		1526	[21, 27, 29, 32, 33, 35-37, 39, 44, 116]
91Cu-9P	715	134	5600			750	[21, 27, 29, 32, 33, 36, 39, 44, 116]
69Cu-17Zn-14P	720	368	7000	0.54(s)		2576	[21, 27, 29, 32, 33, 36, 37, 39, 44, 116]
74Cu-19Zn-7Si	765	125	7170			896	[21, 27, 29, 32, 33, 35-37, 39, 44, 116]
56Cu-27Si-17Mg	742 -770	420 - 422 548[1]	4150 5060(s) 3200(l)	0.75 (s)		1743	[21, 27, 29, 32, 33, 35, 36, 39, 44, 116, 128]
97.25Ca-2.75Si	785	180	1550(s) 1400(l)			279	[128]
84Mg-16Ca	790	272	1380			375	[21, 27, 29, 32, 33, 36, 37, 39, 44, 116]

wt.% Composition (at.%)	T_m (°C)	H_f (kJ/kg)	$\rho_{s/l}$ (kg/m³)	$Cp_{s/l}$ (kJ/kg K)	$k_{s/l}$ (W/m K)	Min $H_{f,v}$ (MJ/m³)	Ref.
47Mg-38Si-15Zn	800	314					[21, 27, 29, 32, 33, 36, 37, 39, 44, 116]
83Cu-17Si	802	267	6090(l)			1626	[128]
80Cu-20Si	803	197	6600	0.50 (s)		1300	[21, 27, 29, 32, 33, 35, 36, 39, 44, 99, 116]
83Cu-10P-7Si	840	92	6880			633	[21, 27, 29, 32, 33, 35, 36, 39, 44, 116]
49Si-30Mg-21Ca	865	305	2250			686	[21, 27, 29, 32, 33, 36, 39, 44, 116]
38.2Al-35.4Si-26.4Fe **($Al_{45}Si_{40}Fe_{15}$ at.%)**	869	562	3360	0.762(s)	8.6-12.8(s)	1888	[72, 75] (2)
56.5Si-43.5Mg **($MgSi_{52.9}$ at.%)**	946 - 947	757 - 774 1212*	1900 - 2000	0.79(s) 0.87	26/20 75	1438	[16, 21, 27-29, 32, 33, 36, 39, 44, 116]
Gold (Au)	961	105	10500			1102	[21]
47.5Ni-40.1Si-12.4Al **($Al_{17}Si_{53}Ni_{30}$ at.%)**	1079	960	4290	0.65(s)	48-51.7(s)	4118	[72, 75] (2)
Copper (Cu)	1077 - 1083	71 (1) 193 - 204	8800 - 8930		350(s)	1698	[16, 32, 35, 37, 48, 116]
Silicon (Si)	1414	1805 - 1926					[35, 48]

(1) The values are considered by the authors out of the expected range.
(2) The composition given in reference [72] is at.% and in reference [75] is wt.%, it may be an error.

The latent heat of fusion for the MPCMs in the range of 300 to 900°C is shown in Fig. 7. The melting temperature of Zinc-based alloys is in the range of 337 to 419°C, approximately, and the average reported heat of fusion is lower than 150 kJ/kg. The Zn-Mg alloy compositions close to the eutectic point are the most studied alloys in this range of temperatures because of their high latent heat of fusion. Al-based alloys were principally investigated in the range of 440 to 660°C, as is shown in Fig. 7. The Mg-based alloys in the same temperature range show the lowest values of latent heat of fusion, whereas the Al-Si have the highest values. The average reported heat of fusion for Al-based alloys is higher than 300 kJ/kg, and the thermal conductivity is higher than Zn-based alloys. As a rule, the alloys with a high content of Si have the higher values of latent heat of fusion, as shown in Fig. 1. Above 700 °C, MPCMs are almost entirely comprised of Cu-based alloys.

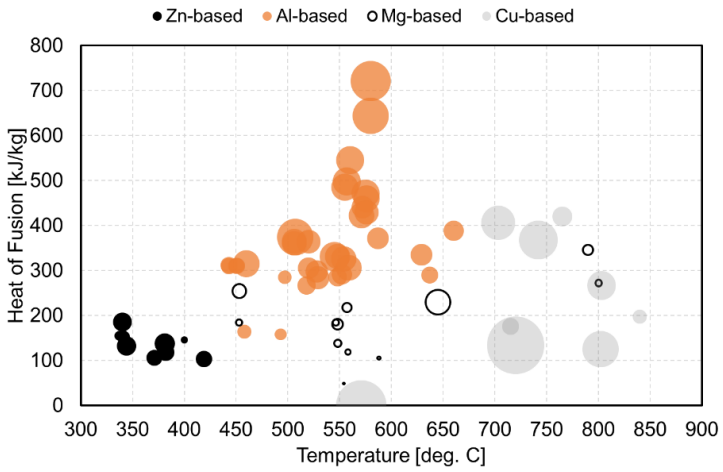

Fig. 7: Latent Heat of Fusion for MPCMs with melting temperature > 300°C. The diameter of the circle represents the Volumetric heat of Fusion

2.2. Medium-Temperature MPCMs, 40°C < Tm < 300°C

In the medium-temperature range of MPCMs, it can be found the low-melting-alloys or fusible alloys composed of such elements as Bi, Pb, Sn, Cd, In, Ga, Zn, Sb. The low-melting-point alloys have extensive applications in the fields of welding, continuous casting simulation, materials processing, electronic and electrical automatic control, and PCMs [129, 130]. In this temperature range, the most notable alloys are commercially known as Cerrolow 117, Cerrolow 136, Wood's metal (also known as Cerrobend or Cerrolow 158). Bismuth is one of the major components of all of them, given the unique characteristic of expansion upon solidification [131]. Wood's metal (50Bi-26.7Pb-13.3Sn-10Cd (wt.%)), proposed by NASA in the 1970s [26], perhaps is the most studied alloy as MPCMs for medium-temperature applications [132, 133]. Wood's alloy was widely used and studied for soldering applications until it was banned for being non-compliant with RoSH due to the content of Pb and Cd [134, 135].

2.2.1. Alloys containing lead and cadmium

Lead (Pb) is listed as one of the chemical elements that represent a significant threat to human life and the environment by the European Union's RoHS (Restriction of Hazardous Substances in Electrical and Electronic Equipment) and the Environmental Protection Agency (EPA). The lead was banned from all new electronic consumer products in the EU from 2006 [134, 135] because of the environmental hazard of electronic waste with Pb. For that reason, in the last 30 years, there have been intensive research and development on lead-free alloys [136-151], and Lead-free solder databases have been created [148, 152, 153]. The primary lead-free candidates to substitute the Pb-Sn eutectic solder are Sn–Ag–Cu near eutectic, Sn–Zn eutectic, and Sn–Bi eutectic alloys. Among them, the strongest candidate is Sn–(3–4)Ag–(0.5–0.9)Cu (wt.%) [137]. Abtew and Selvaduray [136] summarised some of the Pb-free solder alloy compositions proposed for microelectronics assemblies. The studies were focused on the factor that affects the soldering applications as melting point, mechanical properties, wetting characteristics, availability, and cost.

On the other hand, in the microelectronics industry, the cost is a critical factor; therefore, the Pb-free solders must be cost-competitive to maximize the reduction in the overall cost. On an element basis, Pb and Zn are the cheapest metals. Surprisingly, indium (In) is scarce and is more expensive than Ag [139]. El Daly et al. [142, 145, 147] analyzed several binary alloys consist of Sn, Zn, and Bi, finding that the increment of the Bi content decreases their melting point.

The alloys developed as lead-free alloys could be used as PCM for different applications, considering that they met the requirement to be *"safe"* (non-toxic, non-hazardous, non-flammable, non-explosive, non-polluting, non-poisonous). However, the requirements that an alloy needs to serve as a solder are different from the requirements for a PCM. Therefore, it is not easy to find in the new solders database [148, 152, 153] information on the heat of fusion or specific heat of the alloys.

Despite this, there are some recent publications of Lead-free Bi-based alloys as MPCMs for thermal management electronic applications [154-157], a passive thermal management system [158], thermal energy storage and heat sinks [159], and domestic cooking applications [34, 160, 161]. Moreover, there are research works to enhance the relatively low thermal conductivity of the alloys (see Fig. 2a) using graphite foam [162], expanded graphite [12, 155, 162, 163], carbon foam [59, 158], metal foam [157]. Fig. 8 shows the effect of the weight percentage of the Wood's alloy, and the compact density of the composite PCM is the thermal conductivity and latent heat.

Table 2 summarised the thermophysical properties reported in the literature cited for non RoSH compliant alloys, which melt between 40°C and 300°C. The discrepancies in some of the values reported, and the omission of some thermophysical properties can be observed.

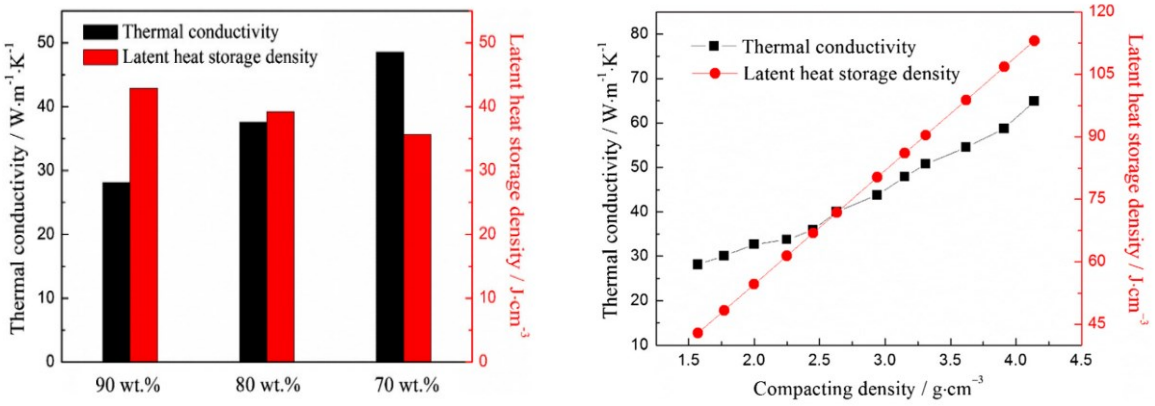

Fig. 8: Thermal conductivity and latent heat storage density of Wood's alloy +Expandable Graphite: a) the composite material with a different mass percentage of Wood's alloy and b) density of the composite with 90 wt.% Wood's alloy. Reprinted from [155] with permission from Elsevier

Table 2: *"Non-RoSH Compliant"* Medium Temperature MPCMs (40°C < Melting Point < 300°C)

Composition (wt.%)	TM (°C)	Hf (kJ/kg)	ρ (kg/m3)	Cp (kJ/kg K)	ks/l (W/m.K)	Min Hf,v (MJ/m³)	Ref.
44.7Bi-22.6Pb-19.1In-8.3Sn-5.3Cd (Cerrolow 117)	47-48	28.5 -36.8 68.2(1)	8860 – 9330	0.15 (s/l) 0.163(s) 0.20	15 16.7(s)	253	[21, 40, 42, 45, 129, 164, 165]
47.5Bi-25.4Pb-12.6Sn-9.5Cd-5In (Indalloy 140)	57- 65	36	9470	0.16(s)	15	341	[21]
49Bi-21In-18Pb-12Sn (Cerrolow 136)	58 - 61	23 – 29.9 90.9(1)	9307 ± 16 (s) 8220(l) 8570 - 9229	0.167 – 0.323 (s) 0.211 ± 0.005 (l) 0.13 (s/l) 0.20 0.721 (l) (1)	7.143 ± 0.028(s) 16.7 - 33.2(s) 10.6(l) 10	218	[21, 26, 39, 40, 42, 45, 129, 154, 158, 164, 166-168]
53.5Bi-19Sn-17Pb-10.5In	60.6/76.2	16.9(1)	9159			155	[129]
51In-33Bi-16Cd	61	25	8000-10040			200	[21, 26, 39, 40, 42, 44]
Potassium (K)	63.2	59.6	664	0.78	54	40	[40, 42]
50Bi-26.7Pb-13.3Sn-10Cd (Cerrolow-158, Cerrobend, Wood's metal)	70.0 – 72.0	29,6 - 45.8 159(1)	8974 - 9620	0.146-0.167(s) 0.20-0.34(s) 0.17 -0.184(l) 0,52	16.7 - 23 (s) 18-19 58.9(1)	266	[21, 26, 30, 34, 39, 40, 42, 45, 129, 155, 164]
52Bi-26Pb-22In	70	29	8000-10103			232	[21, 26, 39, 40, 42, 44]
42.5Bi-37.7Pb-11.3Sn-8.5Cd (Indalloy 160-190)	71/88	34.3	9810	0.146(s)		336	[21, 164]
50Bi-26.7Pb-19.1In-8.3Sn-5.3Cd	72.1	30.4	9582			291	[129]
53Bi-26Sn-21Cd	92.6	2.5(1)	8773			22	[129]
51.6Bi-40.2Pb-8.2Cd	91.5 - 93.0	26.7	10417			278	[129]
50Bi-31Pb-19Sn	94.5	26.4	9590	0.138	16.5	253	[30]
52Bi-30Pb-18Sn (Indalloy 39)	96	34.7	9600	0.151(s) 0.17(l)	13 -24	333	[21, 40, 42]
52.5Bi-32Pb-15.5Sn (Cerrolow 203) 52Bi-32Pb-16Sn	95.0 - 96.9	21.6 - 34.6	9566 - 9714			207	[26, 39, 40, 44, 45, 129, 164, 169]
46Bi-34Sn-20Pb	96.8	26.4 30.5					[169]
50Bi-28Pb-22Sn	95.2 - 100	17.1 – 17.6(1) 32.6	9437			161	[129, 169]
52Bi-30Pb-18Sn	96	22.2 - 36.5					[169]

Composition (wt.%)	TM (°C)	Hf (kJ/kg)	ρ (kg/m3)	Cp (kJ/kg K)	ks/l (W/m.K)	Min Hf,v (MJ/m³)	Ref.
Sodium (Na)	97.8	113.2	850 927(l)	1,27 – 1.38 (l)	69,8 – 86.9 (l) (71)	96	[36, 40, 42, 170]
Eutectic Pb-Bi **($BiPb_{44.7-45.2}$ at.%)** 55Bi-45Pb (Indalloy 255)	123.8 - 126.2	20 - 38.6	9660(l) 9860 - 10460	0.13(s) 0,143 – 0.155(l)	4 12,8- 13,7(l)	193	[21, 26, 34, 35, 39, 40, 113, 164, 169, 171, 172]
58Bi-41Sn-1Pb	134.4	45.9					[169]
51.2Sn-30.6Pb-18.2Cd[2]	145	40.6	8120			330	[129, 164]
Eutectic Sn-Pb **($SnPb_{25.15-25.99}$ at.%)** 63Sn-37Pb 62Sn-38Pb	181 - 183	37.7 - 52.1 104.2[1]	8220 -8400	0.2 (s)	50	310	[34, 35, 142, 151, 160, 169, 173]
60Sn-40Pb	183/190		8520 (s)	0.172 (s)	23.3-26.2 (l)		[173, 174]
62Sn-36Pb-2Ag	179		8410 (s)	0.167 (s)	22.8-26.3 (l)		[173, 174]
85Pb-10Sb-5Sn (Indalloy 233)	245-255	0.9[1]	10360	0.15(s)		9	[21]

[1] The values are considered by the authors out of the expected range.
[2] The wt.% for Pb and Cd was in reference [129].

Liquid metals have also been studied as advanced heat transfer fluids in concentrated solar power plants requiring larger heat-flux densities to improve efficiency and reduce costs [171, 172]. A promising application for liquid Pb-Bi eutectic alloy (55,5Bi-45,5Pb (wt.%) is its use as a coolant for the new generation nuclear reactors [175-178]. In these applications, the compatibility between the liquid Pb-Bi and the structural materials is one of the most severe problems [175-178]. The corrosion of the structural materials used as a container of liquid Pb-Bi alloy is primarily due to the bismuth; the corrosion effect of bismuth is about 40 times faster than the lead [179].

2.2.2. Lead-Free Alloys

Table 3 summarised the thermophysical properties reported in the literature cited for lead-free alloys between 40°C and 300°C. The reported thermophysical properties of medium-temperature MPCMs is limited because they were mainly developed for soldering purposes. There are some omitted and confusing information reported in the published literature of low-melting-point multi-component alloys. Some research groups make efforts to characterize the thermophysical properties and to evaluate the stability of MPCMs. Li and Chung [34] studied the performance of binary alloys Sn-based alloys (including some non-lead-free alloys) for TES applications. They found that the latent heat and thermal conductivity of the Sn-9Zn alloy decreased by approximately 5% after 500 thermal cycles. Meydaneri et al. [180] characterized the thermal conductivity of eutectic alloy Sn-3.5Ag (wt.%) as a function of the temperature. Singh et al. [115], testing bismuth rich Cu-Bi alloys for energy storage and surge protection, pointed out their high thermal stability. Zhou et al. [129] synthesized and systemically investigated the fundamental data of low-melting-point eutectic alloys composed of Bi, Cd, Sn, Pb, and In elements (see Table 3). Shamberger et al. [169] measured the latent heat of fusion of the ternary alloys Sn-Pb-Bi and In-Sn-Bi ternary systems and decouple mixing and electronic contributions (see Table 3). Yang et al. [181] investigated experimentally and numerically the eutectic alloy 31,6Bi-48,8In-19,6Sn (wt.%) as PCM for potential thermal management applications; the alloy showed good repeatability and stability without supercooling. Mawire and Shobo [182] examined the potential of the alloy In–48Sn (wt.%) as PCM for heating applications at medium-temperature; the alloy provides excellent properties as low vapour pressure, thermal stability, congruent melting, and solidification, large volumetric storage capacity, and very small supercooling. Venkitaraj and Suresh [183] experimentally investigated the performance of an organic Solid-Solid/Low Melting Alloy (Bi, Sn, Zn, In) composite PCM for TES applications. The alloy was used as an effective additive for improving the thermal performance of organic PCMs. The thermal storage/ release test showed a reduction of 14.64% and 30.22% in the time taken for total energy compared to pure organic PCM.

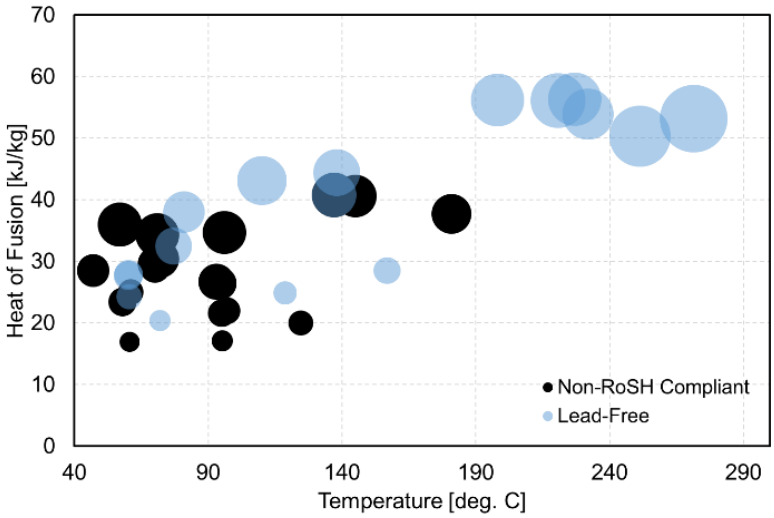

Fig. 9: Latent Heat of Fusion for MPCMs with melting temperature (40 to 300°C). The diameter of the circle represents the Volumetric heat of Fusion

Although thermal energy storage is considered a prospective application for medium-temperature MPCMs [42], the number of studies in this temperature range is reduced compared to high-temperature MPCMs. In this temperature range, the heats of fusion of the metal alloys are below 60 kJ/kg (see Fig. 9), therefore they can be competitive where the minimum volume is a critical requirement, and the weight penalty is acceptable [154].

Table 3 gives the medium-temperature MPCMs, proposed and studied by different authors cited in this review; the thermophysical properties are presented with the range of data found in the reference literature. The alloys in this range of temperatures are mainly Bi-based or Sn-based alloys. Most of these bismuth alloys contain lead and cadmium that are non-RoHS compliant metals. One of the main applications for low melting point alloys is as solder for electronic components where there is enormous pressure for developed Lead-free alloys that replace the Pb-Bi eutectic alloy. Most of the potential MPCM candidates in this range of temperatures were not developed for thermal applications; they are mainly developed for solder applications. Therefore, the thermophysical properties are not studied enough to compare them.

Table 3: "*RoSH Compliant*" Medium Temperature MPCMs (40°C < Melting Point < 300°C)

Composition (wt.%)	TM (°C)	Hf (kJ/kg)	ρ (kg/m3)	Cp (kJ/kg K)	ks/l (W/m.K)	Min Hf,v (MJ/m³)	Ref.
48.8In-31,6Bi-19,6Sn	60.2 ±0.1	27.9 ±0.1	8043 ± 39	0.27 ±0.015(s) 0.297 ±0.003(l)	19.2 ±1.1(s) 14.5 ±0.5(l)	224	[156, 168, 181]
51In-32Bi-17Sn 50.5In-33Bi-16.5Sn	60.1 - 60.7	27.7	8057	0.197	19(s) 20.9	223	[112, 157, 169, 184]
51.34In-33.1Bi-5.56Sn	60.42	24.3	7880 - 8052			191	[129]
Eutectic In-Bi **($InBi_{21.8-22}$ at.%)** 66In-34Bi (Indalloy 162)	72.0 - 72.8	20.4 – 25.0	7990-10000			163	[21, 26, 39, 40, 42, 44, 169]
57.5Bi-25.3In-17.3Sn (57Bi-26In-17Sn)	77.0 - 80.7	32.5 - 47.7	8780(s) 8200(l) 8540 - 8696	0.40(s) 0.88(l) 0.17	35.8(s) 28.8(l) 8.97	285	[129, 166, 169, 184]
54Bi-30In-16Sn	80.9	38	8470			322	[112, 169]
56Bi-40Sn-4In	101.1 - 130.6	3.87(1) 40.6	8525		19.5	33	[35, 129, 185]
67Bi-33In	109 - 110	43.1	8810			380	[112, 169]
Eutectic In-Sn-Zn **($In_{52.7}Sn_{44.9}Zn_{2.4}$ at.%)**	106.5	28.3	7236(s)	0.233(s)	38.8-45.6(s)		[186]

Composition (wt.%)	TM (°C)	Hf (kJ/kg)	ρ (kg/m3)	Cp (kJ/kg K)	ks/l (W/m.K)	Min Hf,v (MJ/m³)	Ref.
Eutectic In-Sn **($InSn_{47.1}$ at.%)** 52In-48Sn	118.7	24.9 - 30.4	7290(s) 7220(l) 7300	0.233(s) 0.416(l)	34 – 40.85 (s) 61.36(l)	182	[112, 164, 169, 173, 182]
60Sn-40Bi (Indalloy 281-338)	138-170	44.4	8120	0.18 (s) 0.21 (l)	30	361	[21]
Eutectic Sn-Bi **($SnBi_{42.95-43.96}$ at.%)** 58Bi-42Sn 57Bi – 43Sn (Indalloy 281)	136.9 - 139.6	40.8 - 49.1	8440 - 8560	0.167(s) 0.201 (l)	21 at 85°C 15.5 -19.0 (s) 15.5(l)	344	[21, 34, 35, 40, 42, 112, 136, 151, 164, 169, 173, 187]
Indium (In)	156.8	28.5 - 28.8	7310 (s) 7030(l)	0.24(s) 0.27(l) 0.23	86(s) 36.4(l)	208	[21, 40, 42, 112, 169, 170]
86Sn-9Zn-5Bi	184.8	55.3			42.6		[34, 35]
Lithium (Li)	179 - 186	433.8 - 663	515 - 534	-4.39	3.98(s) 41.3	223	[27, 40, 42]
90Sn-9Zn-1Bi	196	183.7(1)					[142]
87Sn-9Zn-4Bi	194	163.4(1)					[142]
88Sn-9Zn-3Bi	196.1	63.4			45.5		[34, 35, 142]
Eutectic Sn-Zn **($SnZn_{15.27}$ at.%)** 91Sn-9Zn (Indalloy 201)	198.1 - 199.0	32.5(1) 56.2 - 71.2 191.9(1)	7270 - 7380	0.239(s) 0.272(l)	61(s)	236	[21, 34, 35, 40, 42, 112, 142, 151]
88Sn-9Zn-3Cu	208.1	54.3			54.2		[34, 35]
86Sn-9Zn-5Cu	210.2	48.9			56.8		[34, 35]
95.6Sn-3.5Ag-0.9Cu	217.2	55.1-66.9					[151]
95.5Sn-3.8Ag-0.7Cu	217/220		7405 (s)	0.2207 (s)	27.4-31.6(l)		[112, 173, 174]
Eutectic Sn-Ag **($SnAg_{3.8}$ at.%)** 96.5Sn-3.5Ag	220.7	56.1 - 64,9	7500	0,13 - 0,26	33.0 - 98.4(s) 84,6(l)	421	[112, 151, 173, 180, 188, 189]
Eutectic Sn-Cu **($SnCu_{1.3}$ at.%)** 99.3Sn-0.7Cu	227	56.3 - 62.3	7320 (s) 7310	0.2205 (s)	27.4 - 44.8 (l) 58.9(s)	412	[112, 151, 169, 173, 174, 190]
Tin (Sn)	232	53.9 - 60.5	7280(s) 6940(l)	0.22-0.26	15.1 59 - 73 (s) 29.5(l) 57.0±4.6 (s)	392	[21, 40, 42, 48, 112, 114, 120, 187, 191]
96.5Bi-3.5Zn	251.4	50.3	9340	0.12		470	[34, 35]
Bismuth (Bi)	270. 6 - 271.4	50.9 - 53.9	9790-9800	0.12	8.1 7.3 - 7.5(s) 14(l)	521	[21, 40, 42, 48, 112, 113, 169, 187, 191]

(1) The values are considered by the authors out of the expected range.

2.3. Low-Temperature MPCMs, Tm < 40°C

Low melting point alloys (also called liquid metals) have been investigated for various potentials applications as thermal management in electronic devices [70, 192-196] , management thermal shock in electronics [168], thermal energy storage [192, 197], composite PCMs for solar heat and industrial waste heat recovery application [198], coolant [170, 199-201], thermoelectric generation [202], soft multifunctional composites for wearable electronics [203]. In this range of temperatures, there are gallium and Ga-based alloys; their investigation indicates that the purity level of the alloys has a significant impact on the thermophysical properties [204]. Corrosion problems between the liquid metal and the structural materials are also indicated at low temperatures [199, 205]. The corrosion tests of Gallium and their alloys with metal substrates such as aluminium-alloys, copper-alloy, and stainless steel, indicated that only the stainless steel showed the integral corrosion resistance [199-201, 205]. The supercooling of the Gallium is one of the main drawbacks [206].

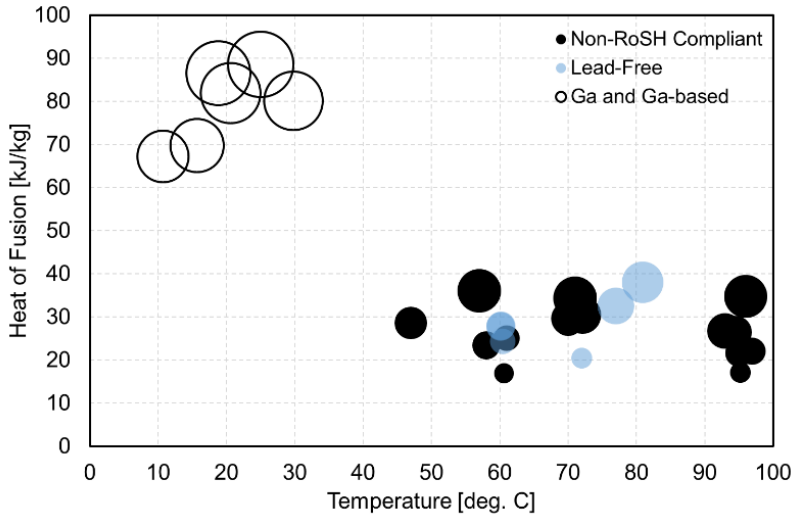

Fig. 10: Latent Heat of Fusion for MPCMs with melting temperature (0 to 100°C). The diameter of the circle represents the Volumetric heat of Fusion

Table 4 lists metallic materials in this low-temperature range. The alloys in this temperature range are Ga-based, the heat of fusion of the Gallium is 80 kJ/kg, and the thermal conductivity approximated 30W/m K. As can be seen from Fig. 10, the Ga-based alloys present a higher heat of fusion and thermal conductivity than the Bi-based alloys (Table 4). In this range of temperatures, the MPCMs have potential impacts in the field of electronics, biomedicine, and beyond.

Table 4: Low-Temperature MPCMs (Melting Point < 40°C)

Composition (wt.%)	TM (°C)	Hf (kJ/kg)	ρ (kg/m3)	Cp (kJ/kg K)	ks/l (W/m K)	Min Hf,v (MJ/m³)	Ref.
Mercury (Hg)	-38.9	11.4	13546(l)	0.14(l)	8.34	154	[21, 40, 42, 170]
66Ga-20.5In-13.5Sn	10.3						[202]
67Ga-20.5In-12.5Sn[(1)]	10.7	67.2	6170		23.4	415	[21, 30, 34, 204]
Eutectic Ga-In **($GaIn_{14.2}$ at.%)** 78.55Ga-21.45In	15.7	69.7	6197 6335(l)	0,404(l)	26,58(l)	432	[21, 30, 34, 170]
82Ga-12Sn-6Zn	18.8	86.5	5961			516	[21, 30, 34]
74Ga-22Sn-4Cd	20.2	75.2	5983			450	[21, 30, 34]
Eutectic Ga-Sn **($GaSn_{8.4}$ at.%)** 86.5Ga-13.5Sn	20.6	81.9	5885			482	[21, 30, 34]
93Ga-5Zn-2Cd	24.6	85	6020			512	[21, 30, 34]
Eutectic Ga-Zn **($GaZn_{3.73}$ at.%)** 96.5Ga-3.5Zn	25	88.5	5946			526	[21, 30, 34]
Cesium (Ce)	28.7	16.4	1796(l)	0.24(l)	17.4(l)	29	[40, 42, 170]
Gallium-gallium antimony	29.8						[26, 39, 40, 44]
Gallium (Ga)	29.8 - 30.0	80.1 - 80.3	5903-5907(s) 5907-6095(l) 5910	0.34 – 0.37(s) 0.39 - 0.40(l) 0.34-0.83	33.5-40.6 (s) 28.1-33.7(l)	473	[21, 26, 39, 40, 42, 44, 45, 168, 170, 192, 207]
Rubidium (Rb)	38.9	25.7	1470	0.36	29.3	38	[40, 42]

[(1)]The composition given in references [21, 30, 34] is 67Ga-20.5In-12.5Zn, which can correspond to a typing error.

3. *Other Thermophysical Properties of MPCMs*

The set of thermophysical properties found in the published literature for MPCMs is generally ~~is~~ not completed, dispersed, conflicted, and subjected to uncertainties. As an example, Stolen and Gronvold [208] presented a review and evaluated the enthalpy of fusion of high purity metals used as enthalpy standards founded that there was a large spread in the literature values mainly due to the differences in experimental techniques and procedures. Several authors [5, 21, 31, 33, 37, 42, 71, 209] brought to light the lack of truthful information on the temperature dependency of the thermo-physical properties of PCMs. As seen in previous sections, the melting point and heat of fusion of MPCMs are well known in general. However, other critical properties, such as density, thermal conductivities, specific heat capacity, viscosity and even heat of fusion, are sometimes missing, contradictory or confusing in the published literature. The eutectic compositions of alloys are specially studied because of their desirable features like single melting temperature, good reliability, and long-term stability under charging and discharging cycles [16]. However, there were many non-eutectic alloys proposed in which the composition of the alloys was not specified, or the nomenclature is confusing (mass weight composition (wt.%), or atomic composition (at.%)).

The absence of an MPCM thermophysical properties handbook, the lack of international standards for characterizations and testing, and the significant variation between sources in measured values of properties have been conducted to the different research groups to employ their methods and resources for characterization of PCMs. Therefore, the majority of the investigations in PCM are focused on characterization and not on the evaluation, design, or guidelines for the potential applications. Thermophysical properties of MPCMs are necessary to produce accurate and reliable LHTES designs using advanced numerical simulations tools, but, unfortunately, the thermophysical data for many alloys are limited. This factor is a significant barrier in developing potential applications because of the need to characterize the PCM spending many resources and time. In summary, there is a definite necessity to generate an "MPCM Handbook," as other authors have already proposed [21] for gathering and summarising the thermophysical properties available for MPCMs. In the next section, the authors compile the temperature dependence of the thermophysical properties and some theoretical predictions needed from an engineering point of view.

3.1. The minimum set of thermophysical properties for MPCMs

All the thermophysical properties should be obtained experimentally; however, some mathematical approximations can estimate the melting point or the expected heat of fusion and the effect on the elements of the alloys. Nowadays, there are software that use the laws of thermodynamics to design and predict the thermophysical properties of alloys [117, 118]. In this section, a compilation of the minimum set of thermophysical properties for MPCMs is intended to be discussed, and the form of the equations generally used to report the dependence with the temperature of the properties required to evaluate, design and study LHTES from an engineering point of view.

3.1.1. Melting Point and Latent Heat of Fusion (Hfit)

The melting point and the latent heat of fusion need to be experimentally obtained using calorimetric methods as differential scanning calorimetry (DSC) or differential thermal analysis (DTA). However, the latent heat of fusion can be predicted for an n-component alloy using Eq.1, the first part of the equation is the contribution of latent heat of pure elements, and the second part is the contribution of specific heat difference between solid and liquid of pure elements [210].

$$H_f = \sum_{i=1}^{n} x_i (H_f)_i \left({}^{T_m}/_{T_i}\right) + T_m \sum_{i=1}^{n} x_i \left(C_{p,l,i} - C_{p,s,i}\right) ln \left({}^{T_m}/_{T_i}\right) \qquad (Eq.\ 1)$$

where x_i is the mole fraction, C_p is the specific heat, T_i is the melting temperature of the element and T_m is the melting temperature of the alloy.

3.1.2. *Density (ρ)*

Vegard's law predicts a linear relationship between molar volume and the molar fraction of constituent elements, and it can be used to calculate the liquid density of metal alloys [169] as Eq.2.

$$\rho_l = \sum_i x_i M_i \Big/ \left(\sum_i x_i \sqrt[3]{M_i / \rho_{li}} \right)^3 \qquad \textit{(Eq. 2)}$$

where ρ_l is the liquid density, x_i is the molar fraction and M_i is the molar mass. Calculated densities are within 2% for those liquid alloys, which have been previously measured experimentally.

The density of pure liquid metals and alloys as a function of temperature can be estimated from an empirical linear equation [211-214]. However, some authors considered the density of melts as weakly nonlinearly dependent on temperature as follows [215]:

$$\rho_l = \rho_0 - c\left(T - T_{ref}\right) + c_1\left(T - T_{ref}\right)^2 \qquad \textit{(Eq. 3)}$$

where ρ_l is the liquid density, ρ_0 is the density at the liquidus temperature when T_{ref} is the melting temperature, c are constants, and T is the temperature. Another form to express the liquid density as linear approximation parameters of its temperature depends on the form of the Eq.4 [216].

$$\rho_l(T) = \rho_l\big(1 - \alpha\,(T - T_l)\big) \qquad \textit{(Eq. 4)}$$

where $\rho_l(T)$ is the liquid density at temperature T, ρ_l is the density at the liquidus temperature, T_l is the liquidus temperature, and α is the volumetric thermal expansion coefficient.

Table 5 and Table 6 present the coefficients of Eq.(3) for the variation of liquid density as a function of the temperature for some MPCMs found in the literature, and Table 7 lists the temperature dependence of liquid density following the Eq.(4).

Table 5: Temperature [K] dependence of Liquid Density (Eq.3)

wt.% Composition	Temp. Range (K)	ρ_0 (kg/m³)	c (kg/m³ K)	c_1 (kg/m³ K²)	T_{ref} (K)	Ref.
Gallium (Ga)	303-1500	6077	0.611		302.9	[214]
	303-410	6112	0.60		302.93	[217]
	410-700	6048	0.70		410	[217]
	303-1274	6269.8	0.6268			[218](1)
	323-773	6262	0.6115			[219]
86.5Ga-13.5Sn 86.3Ga-13.7Sn (8.5 at.% Sn)		6355	0.612			[220]
	323-773	6355	0.6115			[219]
96.5Ga-3.5Zn		6276	0.609			[220]
67Ga-20.5In-12.5Sn		6621	0.874			[220]
	293 – 493	6580	0.776		283.7	[204]
86.3Ga-10.8Sn-2.9Zn	323-773	6332	0.610			[220]
75Ga-25Sn (16.4 at.% Sn)	323-773	6464	0.6120			[219]
75Zn-25Ga		6876	0.471			[123]
75Ga-25Zn		6458	0.599			[123]
50Ga-50Sn (37 at.% Sn)	323-773	6711	0.6123			[219]
50Ga-50Zn		6648	0.515			[123]

wt.% Composition	Temp. Range (K)	ρ_0 (kg/m³)	c (kg/m³ K)	c_1 (kg/m³ K²)	T_{ref} (K)	Ref.
Indium (In)	433.3-1273.5	7318.6	0.699			[218] (1)
	430-1100	7022	0.762		429.7	[214]
52.4In-47.6Bi (33.33 at.% Bi)	365-878	8600.8	0.9571			[221] (2)
Tin (Sn)	323-773	6976	0.6130			[219]
		7370 ± 60	0.82 ± 0.08			[140]
	511-605	7379.5	0.7931			[222] (1)
99.3Sn-0.7Cu	500-1024	7467.0	0.799			[223]
99Sn-1Ag (0.011 at.% Ag)		7396 ± 47	0.813 ± 0.059			[224]
99Sn-1Cu (0.018 at.% Cu)		7504 ± 32	0.838 ± 0.041			[225]
97.1Sn-2.9Cu (0.053 at.% Cu)		7620 ± 32	0.941 ± 0.038			[225]
97Sn-3Ag		7150 ± 70	0.40 ± 0.09			[140]
		6972	0.662		508	[226]
96.5Sn-3.5Ag		6998	0.668		500	[226]
		7480 ± 50	0.72 ± 0.08			[140]
		7398 ± 33	0.804 ± 0.041			[224]
96.15Sn-3.85Ag (96.15 at.% Sn)	495-950	7434.4	0.7013			[221] (2)
96Sn-4Ag		7003	0.688		518	[226]
95.1Sn-2.9Cu (0.087 at.% Cu)		7607 ± 28	0.880 ± 0.03			[225]
95Sn-5Ag (0.055 at.% Ag)		7603 ± 44	1.041 ± 0.055			[224]
94.4Sn-5.6Cu (0.1 at.% Cu)		7675 ± 44	0.889 ± 0.048			[225]
94.5Sn-5.5Zn		6986	0.722		480	[226]
92.6Sn-4.7Ag-2.8Cu (5 at.% Ag-5 at.% Cu)	550-1000	7265 ± 23	0.565 ± 0.029			[227]
91.9Sn-6.5Ag-1.6Cu (7 at.% Ag-3 at.% Cu)	550- 1000	7313 ± 13	0.581 ± 0.016			[227]
91.5Sn-8.5Zn		6975	0.725		478	[226]
91.2Sn-8.8Zn	473-1157	7291.2	0.658			[223]
90.8Sn-9.2Ag (0.1 at.% Ag)		7534 ± 43	0.864 ± 0.053			[224]
90Sn-10Ga (84.1 at.% Sn)	323-773	7137	0.6128			[219]
90Sn-10Pb		7540 ± 40	0.72 ± 0.06			[140]
89.5Sn-10.5Zn		6963	0.745		488	[226]
88.2Sn-11.8Cu (0.2 at.% Cu)		7668 ± 57	0.709 ± 0.056			[225]
86.9Sn-11.3Bi-1.7Cu		8087	0.909			[228]
84.7Sn-9.6Ag-5.7Cu (10 at.% Ag-10 at.% Cu)	650-1100	7584 ± 18	0.643 ± 0.021			[227]
81.5Sn-18.5Ag (0.2 at.% Ag)		7889 ± 46	0.871 ± 0.051			[224]
81.3Sn-18.7Cu (0.3 at.% Cu)		8022 ± 56	0.973 ± 0.053			[225]
76.4Sn-14.9Ag-8.8Cu (15 at.% Ag-15 at.% Cu)	750-1150	7863 ± 32	0.670 ± 0.035			[227]
74.7Sn-21.9Bi-3.3Cu		8893	1.27			[228]
74.5Sn-20.3Ag-5.1Cu (21 at.% Ag-9 at.% Cu)	650-1100	7560 ± 33	0.612 ± 0.037			[227]
75Sn-25Ga (63.8 at.% Sn)	323-773	6976	0.6127			[219]

wt.% Composition	Temp. Range (K)	ρ_0 (kg/m³)	c (kg/m³ K)	c_1 (kg/m³ K²)	T_{ref} (K)	Ref.
72.5Sn-27.5Bi	447-745	7940	0.778		447	[229]
72Sn-28Ag (0.3 at.% Ag)		8167 ± 46	0.831 ± 0.048			[224]
67.5Sn-20.4Ag-12Cu (20 at.% Ag-20 at.% Cu)	800-1200	7995 ± 39	0.706 ± 0.039			[227]
65.1Sn-34.9Cu (0.5 at.% Cu)		8248 ± 56	0.837 ± 0.049			[225]
63.3Sn-31.8Bi-4.8Cu		8957	0.962			[228]
61.9Sn-38.1Pb	400-1040	8472	0.810			[213]
61.6Sn-38.4Ag (59.3 at.% Sn)	715-940	8473	0.8143			[221] (2)
60Sn-40Pb		8450 ± 20	0.76 ± 0.02			[140]
58.1Sn-26.4Ag-15.5Cu (25 at.% Ag-25 at.% Cu)	750-1200	8346 ± 74	0.741 ± 0.074			[227]
57Sn-43Bi	425-745	8730	1.390		412	[229]
		8155.3 ± 16.3	1.018 ± 0.020	(2.58 ± 0.33)E-4	439.3	[215]
55.7Sn-35.4Ag-8.9Cu (35 at.% Ag-15 at.% Cu)	700-1200	8491 ± 26	0.745 ± 0.027			[227]
52.6Sn-41.1Bi-6.3Cu		9413	1.02			[228]
52.4Sn-47.6Ag (0.5 at.% Ag)		8982 ± 197	1.322 ± 0.190			[224]
Bismuth (Bi)	553-1273	10726	1.221			[230] [113]
	545-1500	10028	1.213		544.55	[231]
65.9Bi-24.1Sn-10Cu		9611	0.560			[228]
67.4Bi-32.6Sn (53.97 at.% Bi)		8931.7 ± 17.9	1.082 ± 0.022	(1.53 ± 0.24)E-4	434.3	[215]
	433-923	9374	1.0179			[221] (2)
67Bi-33In (52.73 at.% Bi)	382-883	9257.4	1.0533			[221] (2)
60Bi-40Sn	452-745	9220	1.487		452	[229]
58.1Bi-33Sn-8.8Cu		9376	0.612			[228]
58Bi-42Sn (43.96 at.% Bi) 57.5Bi-42.5Sn		8637.1 ± 17.3	1.035 ± 0.021	(1.61 ± 0.19)E-4	411.2	[215]
	409-922	9025.8	0.9554			[221] (2)
	407-1258	9068.4	0.916			[223]
56Bi-44Pb 55.5Bi-44.5Pb (LBE)	400-680	10080	1.15		398	[229]
	400-1225	10922	1.096			[213]
	403-1273	11096	1.324			[230]
	403 – 1273	11065	1.293			[113]
	404-678	11054.5	1.3366			[232]
	404-678	10522.4	1.3366		398.1	[232]
		1103	1.2246			[233]
49.9Bi-42.5Sn-7.6Cu		9793	1.14			[228]
46Bi-29Pb-25Sn	370-650	9690	0.892		368	[229]
Lead (Pb)	601-1900	11367	1.194			[230]
	601-1823	11441	1.2795			[113]
		11471	1.32			[234]
	601-2000	10656	1.239		600.61	[231]

wt.% Composition	Temp. Range (K)	ρ_0 (kg/m³)	c (kg/m³ K)	c_1 (kg/m³ K²)	T_{ref} (K)	Ref.
89.4Pb-10.6Sb (16.75 at.% Sb)	573-923	10840	1.13			[234]
71.9Pb-28.1Sb (40 at.% Sb)	573-923	9980	1.08			[234]
53.2Pb-46.8Sb (60 at.% Sb)	573-923	8990	0.97			[234]
Zinc (Zn)		6580	0.98		692.7	[235]
	692-910	6559	0.884		696.7	[214]
		7157	0.450			[123]
	429.9-480.8	7872.9	1.3813			[236]
87.9Zn-12.1Al (75 at.% Zn)	873-1023	6290	1.24			[237]
90Zn-Ga		7008	0.426			[123]
70Zn-30Al (49 at.% Zn)	873-1023	5390	1.35			[237]
Antimony (Sb)		6982	0.75			[234]
	900-1300	6467	0.608		899	[231]
84.1Sb-15.9Pb (90 at.% Sb)	573-923	7691	0.82			[234]
Magnesium (Mg)		1590	0.26		922	[235]
63.5Mg-31.4Al-5Zn	773-973	2636.6	0.94			[238]
60.7Mg-39.3Al (63.2 at.% Mg)	723-1053	2441.3	0.80			[238]
50.2Mg-49.8Al (52.8 at.% Mg)	723-1053	2726.0	0.99			[238]
Aluminium (Al)	723-1053	2674.3	0.31			[238]
		2380	0.35		933.5	[235]
94.7Al-5.3Zn	773-1023	7168.7	1.700			[223]
88Al-12Si	858-1700	2603	0.241			[213]
66.8Al-33.2Zn (17 at.% Zn)	923-1023	4490	1.90			[237]
63.8Al-36.2Mg (38.6 at.% Mg)	723-1053	2772.1	0.80			[238]
60.8Al-34.6Mg-4.5Zn	773-973	2965.2	0.93			[238]
47.4Al-47.7Mg-5Zn	773-973	2882.4	1.06			[238]
Calcium (Ca)	1085-1156	2357	0.8851			[222] (1)
Silver (Ag)	1235-1600	9294	0.877		1234.93	[231]
95.8Ag-4.2Sn	507-1276	7425.5	0.722			[223]
Silicon (Si)		2530	0.35		1683	[235]
Nickel (Ni)	1728-2500	7861	0.988		1728	[231]

(1) Coefficients obtained from the data provided.
(2) Coefficients obtained from digitalized graphic data provided.

Table 6: Temperature [°C] dependence of Liquid Density (Eq.3)

wt.% Composition	Temp. Range (°C)	ρ_0 (kg/m³)	c (kg/m³ °C)	T_{ref} (°C)	Ref.
95Sn-5Zn (91.3 at.% Sn)		7131	0.7872	0	[239]
91Sn-9Zn (84.8 at.% Sn)		7097	0.7699		[239]
	513-723	7348	0.758		[240]
85.7Sn-14.3Cd (85 at.% Sn)		7252	0.7659		[239]

wt.% Composition	Temp. Range (°C)	ρ_0 (kg/m³)	c (kg/m³ °C)	T_{ref} (°C)	Ref.
67.7Sn-32.3Cd (66.5 at.% Sn)		7389	0.7571		[239]
64.5Sn-35.5Zn (50 at.% Sn)		6988	0.8221		[239]
51.4Sn-48.6Cd (50 at.% Sn)		7566	0.8163		[239]
95Cd-5Pb (2.8 at.% Pb)		8458	1.1571		[239]
88.3Cd-11.7Sn (11.18 at.% Sn)		8115	0.9994		[239]
83Cd-17Pb (10 at.% Pb)		8669	1.1308		[239]
74Cd-26Sn (25 at.% Sn)		7964	1.1293		[239]
61.9Cd-38.1Pb (25 at.% Pb)		9140	1.1751		[239]
50Cd-50Pb (35.2 at.% Pb)		9457	1.1995		[239]
94.3Pb-5.7Cd (90 at.% Pb)		10844	1.2375		[239]
84.7Pb-15.3Cd (75 at.% Pb)		10518	1.3035		[239]
82.5Pb-17.5Cd (71.9 at.% Pb)		10438	1.2747		[239]
77Pb-23Cd (64.5 at.% Pb)		10278	1.3168		[239]
64.8Pb-35.2Cd (50 at.% Pb)		9852	1.1921		[239]
99.5Zn-0.5Pb (0.16 at.% Pb)		6966	0.9566		[239]
98.4Zn-1.6Pb (0.52 at.% Pb)		7010	1.011		[239]
83.2Zn-16.8Sn (10 at.% Sn)		6987	0.8577		[239]
62.3Zn-37.7Sn (25 at.% Sn)		6886	0.771		[239]

(1) Coefficients obtained from data provided
(2) Coefficients obtained from digitalized graphic data provided

Khairulin and Stankus [241] proposed the following equation for the temperature dependence of the melt density over the range from the eutectic temperature 456 K to 1040 K for the eutectic alloy 61.9Sn-38.1Pb (26.07 at % Pb) based on experimental data:

$$\rho = 8121.2 - 0.9176\,(T - 456.6) + 1.8691x10^{-4}\,(T - 456.6)^2 - 6.789x10^{-8}(T - 456.6)^3 \quad \textit{(Eq. 5)}$$

Table 7: Temperature dependence of Liquid Density (Eq.4)

wt.% Composition	ρ_l (kg/m³)	α (1/°C)	T_l (°C)	Ref.
Aluminium (Al)	2374	12.4E-5	661	[216]
Copper (Cu)	7970	9.0E-5	1084	[216]
97.8Cu-2.2Al (5 at.% Al)	7809	9.6E-5	1080	[216]
95.5Cu-4.5Al (10 at.% Al)	7324	9.7E-5	1070	[216]
91.5Cu-8.5Al (18 at.% Al)	7010	10.3E-5	1032	[216]
87.6Cu-12.4Al (25 at.% Al)	6700	11.9E-5	1049	[216]
84.6Cu-15.4Al (30 at.% Al)	6220	11.4E-5	1040	[216]
82.1Cu-17.9Al (34 at.% Al)	6010	12.1E-5	1022	[216]
77.9Cu-22.1Al (40 at.% Al)	5640	11.5E-5	960	[216]
74.2Cu-25.8Al (45 at.% Al)	5420	10.8E-5	900	[216]
70.2Cu-29.8Al (50 at.% Al)	5299	10.1E-5	850	[216]
65.8Cu-34.2Al (55 at.% Al)	4938	10.0E-5	790	[216]

61.1Cu-38.9Al (60 at.% Al)	4345	10.9E-5	700	[216]
55.9Cu-44.1Al (65 at.% Al)	4238	10.8E-5	620	[216]
52.8Cu-47.2Al (67.8 at.% Al)	3881	8.13E-5	591	[216]
44Cu-56Al (75 at.% Al)	3691	8.4E-5	580	[216]
32.7Cu-67.3Al (82.9 at.% Al)	3239	9.5E-5	550	[216]
20.7Cu-79.3Al (90 at.% Al)	2966	9.7E-5	600	[216]
95.5Cu-4.5Al (95 at.% Al)	2575	12.1E-5	640	[216]
wt.% Composition	ρ_l **(kg/m³)**	α **(1/K)**	T_l **(K)**	**Ref.**
97.6Pb-2.4Mg (83.06 at.% Pb)	9563 ± 27	(11.7±0.2)E-5	522.7	[242]
90.3Pb-9.6Mg (52.46 at.% Pb)	7027 ± 17	(12.9±0.4)E-5	730	[242]
81Pb-19Mg (33.45 at.% Pb)	5256 ± 15	(14.6±0.8)E-5	823	[242]
66.8Pb-33.2Mg (19.11 at.% Pb)	3773 ± 10	(14.7±0.6)E-5	740.2	[242]

Khairulin and Stankus [241] recommended an expression for the density of the liquid lead-tin system depending on the temperature and concentration. The temperature range from liquidus line to 750 K, and the composition interval of 0–33.88 at.% Pb is as follows:

$$\rho = 7359.5 + 47.6551C - 0.10063C^2 - (0.74284 + 5.8927E - 3C)T \qquad (Eq.\ 6)$$

where C is the Pb content in the alloy in at.%, T is the absolute temperature, and ρ is the density in kg/m^3. Stankus et al. [221] measured the density of bismuth-tin and silver-tin binary alloys; the typical results of measuring the density of alloys versus temperature follows a linear behaviour.

The density of solid alloys as a function of temperature can be estimated from thermal expansion data with the following equation [212]:

$$\rho_s = {}^{\rho}/_{\alpha\, T} \qquad (Eq.\ 7)$$

where α is the linear thermal expansion coefficient, and T is the temperature. Semi-empirical analyses of the thermal expansion of crystalline materials revealed the relationship between the mean coefficient of linear thermal expansion (α_m) and the melting temperature [212]:

$$T_m \alpha_m \approx 0.0222 \qquad (Eq.\ 8)$$

3.1.3. Specific Heat Capacity (Cp)

The specific heat capacity depends on the number of species in the system, and it can be estimated for a liquid alloy ($C_{p,l}$) from the elemental heat capacities of the components in the alloy by using the Kopp-Neuman rule of mixtures [212]:

$$C_{p,l} = \sum_{i=1}^{n} x_i (C_p)_{li} \qquad (Eq.\ 9)$$

where x_i is the atomic fraction of element *i* in the alloy.

This equation provides a reasonable value of liquid specific heat capacity (±3%) of the alloy due to the insignificant changes in the liquid specific heat capacity with the temperature of the elements. In the mushy zone, solid-liquid range, the specific heat capacity presents significant changes with heating or cooling rates [212].

Table 8 illustrates the coefficients for the empirical second-order polynomial equations of the variation of specific heat with the temperature published for some metal alloys are as follows:

$$c_{p,l} = a + bT + cT^2 + dT^{-2} \qquad (Eq.\ 10)$$

Table 8: Temperature dependence of Specific Heat (Eq.10)

wt.% Composition	Temp. Range (°C)	a (kJ/kg °C)	b (kJ/kg °C²)	c (kJ/kg °C³)	d (kJ°C /kg)	Ref.
96.48Al-3.52Mg	30 -500	0.69058	4.57306E-4	-		[75]
90.05Al-4.91Cu-5.04Zn	30 -500	0.94403	-5.82262E-4	2.06044E-6		[75]
89.65Al-10.35Cu	30 -500	0.84999	9.19982E-5	-		[75]
80.3Al-19.7Si	30 -500	1.11513	5.0358E-4	-		[75]
79.86Al-10.3Cu-9.84Zn	30 -500	0.96562	-0.00149	2.32876E-6		[75]
79.1Al-20.9Cu	30 -500	0.84908	2.91358E-4	-		[75]
69.88Al-30.12Cu	30 -500	0.59075	7.57875E-4	-		[75]
69.1Al-20.50Cu-10.45Zn	30 -500	0.71747	-0.00131	2.19015E-6		[75]
62.92Al-26.98-10.10Zn	30 -500	0.73675	-0.00135	3.221E-6		[75]
59.87Al-40.13Cu	30 -500	0.54948	-1.16513E-4	-		[75]
wt.% Composition	**Temp. Range (K)**	a **(kJ/kg.K)**	b **(kJ/kg.K²)**	**c (kJ/kg.K³)**	**d (kJ.K /kg)**	**Ref.**
Bismuth (Bi)	545-1300	118.2	5.934E-3	-	7.183E6	[113]
55.5Bi-44.5Pb	430-605	164.8	-3.94E-2	1.25E-5	-4.56E5	[113]
Lead (Pb)	601-1300	175.1	-4.923E-2	1.544E-5	-1.524E6	[113]

3.1.4. Thermal Conductivity (k)

The thermal conductivity can be described by a second-order polynomial as a function of the temperature as follows:

$$k = k_o + a(T - T_{ref}) + b(T - T_{ref})^2 \qquad (Eq.\ 11)$$

where k_o is the thermal conductivity at the melting temperature when $T_{ref} = T_m$, a and b are constants. Lattice Monte-Carlo numerical method can be used to estimate the thermal conductivity of two and three-phase materials [243]. Table 9 summarizes the temperature dependence of thermal conductivity found in the literature (Eq.11) and the coefficients obtained from thermal conductivity data.

Table 9: Temperature dependence of Thermal Conductivity (Eq.11)

wt.% Composition	Temp. Range (K)	k_o (W/m² K)	a (1/ K)	b (1/ K²)	T_{ref} (K)	Ref.
Gallium (Ga)	350-550	1.123	0.09844	-5.629E-5		[244]*
	310-800	7.6 ± 0.4	0.0792 ± 0.01	-(2.6 ± 1)E-5		[245]
	-700	30.2	0.041		302.93	[217]
	303-850	28.403	0.071896		302.914	[246]
67Ga-20.5In-12.5Zn	283.7 – 600	23.4	0.0614	4.9e-5	283.7	[204]
Indium (In)	430-1300	36.493	0.029185		429.748	[246]
	470-1275	13.06	0.05368	-1.66E-5		[247]
	440-800	31.5 ± 1.6	0.0428 ± 0.0004		440	[245]
80.53In-19.47Sn		6.60	0.0582	-1.630E-5		[248]

wt.% Composition	Temp. Range (K)	k_o (W/m² K)	a (1/ K)	b (1/ K²)	T_{ref} (K)	Ref.
49.29In-48.4Sn-2.31Ag	313-373	29.45	0.3646	-6.75E-4		[249]*
Tin (Sn)	507-2000	28.037	0.023397		505.8	[246]
	505-1200	13.90	0.02868			[250]
	313-393	81.136	-0.0463			[251]**
	373-473	89.22	-0.061			[252]**
	373-473	67.2	-0.066		373	[253]*
99.3Sn-0.7Cu (1.3 at.%Cu)	400-700	410.53	-0.0386	-4.408E-5		[254]**
99Sn-1Mg	333-463	94.793	-0.0693			[252]**
99.5Sn-0.5Al	363-493	83.5	-0.10615		363	[253]*
98Sn-2Mg	323-463	119.78	-0.1077			[252]**
98Sn-2In (2.1 at.%In)	323-473	104.95	-0.1398	9.769E-5		[190]**
98Sn-2Mg	323-463	14.135	0.4373	-6.93E-4		[189]*
97.8Sn-2.2Al	323-492	92.463	0.094	-2.337E-4		[255]**
	323-493	98.8	-0.10882		323	[253]*
96.5Sn-3.5Ag (s)*	323 – 483	129.92	-0.1026	2.14E-5		[180]
95.6Sn-3.5Ag-0.9Cu	313-473	67.899	-0.0102	-5.641E-5		[249]*
95Sn-5Pb	323-423	76.269	-0.0392			[256]**
94Sn-6Mg	323-463	112.04	-0.0656			[252]**
94Sn-4Ag-2In	323-473	71.423	-0.0182			[190]**
93.9Sn-4Ag-2.1In (4.4 at.% Ag -2.1 at.%In)	322-473	65.71	0.0116	-3.77E-5		[190]**
90Sn-10Ag	313-473	153.22	-0.2093			[251]**
90Sn-10Bi	313-393	49.465	-0.0358			[251]**
90Sn-10Cu	313-473	93.764	-0.061			[251]**
90Sn-10In	313-373	99.117	-0.0849			[251]**
90Sn-10Zn	313-433	76.011	-0.0436			[251]**
89Sn-6Sb-5Ag	313-493	49.14	0.07667	-1.821E-4		[249]*
86Sn-14Zn	323-463	85.69	-0.0625		323	[257]*
76Sn-22Ag-2In	323-473	78.02	-0.045			[190]**
75Sn-25Al	323-494	126.27	0.1677	-3.946E-4		[255]**
	323-493	235.5	-0.27647		323	[253]*
75Sn-25Bi	323-383	31.888	-0.0151			[251]**
70Sn-10Ag-20In	323-453	114.04	-0.129	7.388E-5		[258]*
65.95Sn-34.05In		8.11	0.0427	-0.886E-5		[248]
61.9Sn-38.1Pb	323-423	78.904	-0.0528			[256]**
60Sn-40Pb	323-423	79.252	-0.0559			[256]**
58Sn-40Ag-2In	323-473	73.161	-0.0411			[190]**
57.16Sn-42.8Bi-0.04Cu	313-393	26.97	0.06501	-2.018E-4		[249]*
55Sn-25Ag-20In	323-453	114.15	-0.1565	1.187E-4		[258]*

wt.% Composition	Temp. Range (K)	k_o (W/m² K)	a (1/ K)	b (1/ K²)	T_{ref} (K)	Ref.
53Sn-40Cd-7Sb (41.39 at.% Cd – 6.69 at.% Sb)	323-443	88.511	-0.0892			[259]
52.9Sn-45.8Bi-1.3Zn (32 at.% Bi-2.99 at.% Zn)	313-393	82.045	-0.1099			[259]
51.1Sn-48.4In-0.5Cu (49 at.% In – 1 at.% Cu)	318-378	118.33	-0.1299			[259]
50.07Sn-49.93In		6.30	0.0509	-1.370E-5		[248]
50Sn-50Al	323-493	202.88	0.0778	-3.677E-4		[255]**
	323-493	191.7	-0.29235		323	[253]*
50Sn-50Zn	323-463	97.31	-0.1093		323	[257]*
Bismuth (Bi)	545 – 1000	6.55	0.01			[230]
	464 – 1000	7.34	0.0095			[113]
	545-1110	13.199	0.01147		544.55	[260]
	573-823	6.88	0.0059	3.214E-6		[261]*
	313-373	14.866	-0.0208			[251]**
	545-970	8.2	0.0058	3.89E-6		[262]
98.2Bi-1.5Zn-0.3Al (4.5 at.%Zn-2 at.% Al)	323-513	21.723	-0.0425	3.5987E-5		[263]*
97.9Bi-2Zn-0.1Al	323-513	15.403	-0.0083			[264]**
93.1Bi-6.6Zn-0.3Al (18 at.%Zn-2 at.% Al)	323-513	25.984	-0.0416	2.8664E-5		[263]*
87.5Bi-12.1Zn-0.3Al (30.1 at.%Zn-2 at.% Al)	323-513	37.266	-0.0735	5.7145E-5		[263]*
56.24Bi-42.73Sn-1.03Ag	313-393	34.851	-0.0301			[249]*
55.5Bi-44.5Pb	403 – 1100	3.61	0.01517	-1.74E-6		[230]
	403 – 1073	3.28	0.01617	-2.305E-6		[113]
	423-773	0.3087	0.0251	-9.167E-6		[261]*
97Cd-3Zn (5 at.% Zn)	373-533	123.03	-0.0709			[265]**
95Cd-5Pb	323-513	124.11	-0.0781			[266]**
82.7Cd-17.3Zn (26.5 at.% Zn)	373-533	113.08	-0.0592			[265]**
Lead (Pb)	601 – 1300	9.2	0.011			[113, 230]
	623-873	8.44	0.0597	-3.286E-5		[261]*
	620-730	15.95	0.0128		600	[267]
	601-1000	7.665	0.016			[268]
	602-1150	16.093	0.0078526		600.61	[246]
	323-593	38.924	-0.0111			[266]**
95Pb-5Sn	323-423	57.919	-0.0505			[256]**
95Pb-5Cd	323-513	51.32	-0.0337			[266]**
90Pb-10Sn	323-423	67.341	-0.0661			[256]**
88Pb-12Cd	323-513	63.066	-0.0422			[266]**
80Pb-20Sn	323-423	64.783	-0.0493			[256]**
65Pb-35Sn	323-423	68.732	-0.044			[256]**
50Sn-50Pb	323-423	78.151	-0.0615			[256]**

wt.% Composition	Temp. Range (K)	k_o (W/m² K)	α (1/K)	b (1/K²)	T_{ref} (K)	Ref.
50Cd-50Pb	323-513	70.117	-0.0413			[266]**
Zinc (Zn)	323-688	135.96	-0.1055		323	[257]*
99.2Zn-0.8Al (98 at.%Zn-2 at.% Al)	323-513	132.9	-0.136	6.508E-5		[263]*
97.8Zn-2.2Cd (1.3 at.% Cd)	373-533	107.79	-0.0579			[265]**
97.8Zn-1.3Al-1Bi	323-623	175.78	-0.0608			[269]**
80Zn-20Sn	323-463	108.25	-0.1407		323	[257]*
56.2Zn-43.2Bi-0.6Al (79 at.%Zn-2 at.% Al)	323-513	40.03	0.055	-1.056E-4		[263]*
Aluminium (Al)	380-600	249.74	0.0165	-9.219E-5		[270]*
	423-923	302.9	-0.1888		423	[253]*
92.6Al-7.4Cu	298 -775	61.03	0.4558	-0.0004		[125]
75Al-25Sn	323-493	136.13	0.667	-1.124E-3		[255]**
Silver (Ag)	313-373	511.48	-0.2397			[251]**
72Ag-20In-8Sn	323-453	55.78	0.0581	-1.612E-4		[258]*
71Ag-27Sn-2In	323-473	55.728	-0.0234			[190]**
65Ag-20In-15Sn	323-453	35.43	0.172	-2.836E-4		[258]*
60Ag-38Sn-2In	323-473	73.816	-0.058			[190]**
45Ag-20In-35Sn	323-453	65.614	0.053	-1.296E-4		[258]*
44.1Ag-38.8Sn-17.1Bi (50 at.% Ag – 10 at.% Bi)	313-393	149.63	-0.1866			[259]
Copper (Cu)	1358-1700	150.49	0.070410		1357.77	[246]
51.7Cu-48.3Al	298-775	78.24	0.1116	-8E-5		[125]
Silicon (Si)	1690-1945	54.702	0.00153		1687.0	[260]
Nickel (Ni)	1730-2000	54.182	0.020970		1728	[246]
Iron (Fe)	1815-2050	36.349	0.0096207		1811	[246]
Titanium (Ti)	587-800	18.4 ± 0.9	0.0266 ± 0.0003		587	[245]
Platinum (Pt)	375-600	68.965	1.818E-4	8.727E-6		[270]*
Cobalt (Co)	1769-1903	29.494	0.08781		1768.15	[260]
wt.% Composition	**Temp. Range (°C)**	**k_o (W/m² K)**	**α (1/°C)**	**b (1/°C ²)**	**T_{ref} (K)**	**Ref.**
Tin (Sn)	250-600	24.31	0.0155	1.481E-5		[187]*
Bismuth (Bi)	300-600	12.397	0.0033	9.467E-6		[187]*
57Bi-43Sn	150-600	13.59	0.017	1.752E-6		[187]*
96.48Al-3.52Mg	30 -500	111.11	0.0888			[75]
90.05Al-4.91Cu-5.04Zn	30 -500	152.63	0.07515			[75]
89.65Al-10.35Cu	30 -500	181.69	-0.031			[75]
80.3Al-19.7Si	30 -500	183.36	0.07343			[75]
79.86Al-10.3Cu-9.84Zn	30 -500	129.49	0.01033			[75]
79.1Al-20.9Cu	30 -500	165.91	0.0047			[75]
69.05Al-20.50Cu-10.45Zn	30 -500	99.99	-0.02373			[75]

wt.% Composition	Temp. Range (K)	k_o (W/m² K)	a (1/ K)	b (1/ K²)	T_{ref} (K)	Ref.
62.92Al-26.98-10.10Zn	30 -500	98.39	0.02264			[75]
69.88Al-30.12Cu	30 -500	120.3	0.0816			[75]
59.87-40.13Cu	30 -500	112.67	-0.0513			[75]

* Coefficients obtained from data provided, ** Coefficients obtained from digitalized graphic data provided

3.1.5. Viscosity (μ)

The laws of Arrhenius and Andrade are the most famous temperature-dependent viscosity laws. Andrade derived a semi-empirical for the viscosity in metals as follows:

$$\mu\, v^{1/3} = A\, exp\left(C/_{vT}\right) \qquad (Eq.\ 12)$$

where v is the specific volume, A and C are constants, and T is the absolute temperature. Modification to Andrade's equation proposes [212, 271]:

$$\mu_m = 1.7x10^{-7}\rho^{2/3}T_m^{1/2}M^{-1/6} \qquad [Pa\ s] \qquad (Eq.\ 13)$$

where ρ is the density, M is the atomic mass, and T_m is the melting point in degrees Kelvin. Table 10 reports the coefficients of Eq. 12 for temperature-dependent viscosity following Andrade's law.

Table 10: Constants of Dynamic Viscosity as Andrade' Equation (Eq.12)

wt.% Composition	A	C	Ref.
Tin (Sn)	2750	88.49	[211]
85Sn-15Pb	2530	94.96	[211]
70Sn-30Pb	2540	93.28	[211]
61.9Sn-38.1Pb	2530	92.78	[211]
60Sn-40Pb	2478	94.66	[211]
Lead (Pb)	2540	86.30	[211]
98Pb-2Sb	2428	89.561	[272]
95Pb-2.5Sb-2.5Sn	2502	88.255	[272]
93.1Pb-6.9Sb	2368	91.030	[272]
90Pb-5Sb-5Sn	2469	89.728	[272]
90Pb-10Sn	2470	90.00	[211]
89.2Pb-10.8Sb	2373	91.969	[272]
84.8Pb-10.2Sb-5Sn	2242	96.327	[272]
80Pb-10Sb-10Sn	2192	98.848	[272]
80Pb-20Sn	2400	93.14	[211]
70Pb-30Sn	2460	92.71	[211]
60Pb-40Sn	2470	93.07	[211]
50Pb-50Sn	2500	93.61	[211]

Arrhenius' law proposed the following equation for the viscosity using the activation energy E_a:

$$\mu = \mu_0 exp\left({}^{E_a}/_{RT}\right) \qquad (Eq.\ 14)$$

Here, the constants E_a is the activation energy of the viscous fluid, R is the gas constant = 8.3144 J/mol.K and μ_0 is the pre-exponential factor. Table 11 displays the coefficients of Eq. 14 for temperature-dependent viscosity following Arrhenius's law.

Mudry et al. [273] measured the viscosity of Bi-Zn liquid alloys using the oscillating crucible method and proposed a modification of the Arrhenius' equation:

$$\mu(T) = \mu_0 exp\left({}^{E_a}/_{RT}\right)\epsilon^{-y} \qquad [Pa\ s] \qquad (Eq.\ 15)$$

where ϵ^{-y} term describes the divergence of viscosity introduced by concentration fluctuations near the critical temperature (ϵ << 1).

Table 11: Temperature dependence of Dynamic Viscosity as Arrhenius' law (Eq.14)

wt.% Composition	η_0 (mPa.s)	E_a (J/mol)	${}^{E_a}/_{R}$ (K)	Ref.
Gallium (Ga)	0.358	3906.7	470.1	[123]
	0358	3906.7		[219]
86.3Ga-10.8Sn-2.9Zn	0.376	3824.3		[220]
86.3Ga-13.7Sn (8.5 at.% Sn)	0.342	4295.8		[219]
75Ga-25Sn (16.4 at.% Sn)	0.310	5290.2		[219]
75Ga-25Zn	0.372		815.3	[123]
67Ga-20.5In-12.5Zn	0.4352		469.8	[204]
50Ga-50Zn	0.377		1159.4	[123]
50Ga-50Sn (37 at.% Sn)	0.254	7148.1		[219]
86.5Ga-13.5Sn	0.342	4295.8		[220, 274]
96.5Ga-3.5Zn	0.367	3953.4		[220]
67Ga-20.5In-12.5Sn	0.444	3827.0		[220]
Tin (Sn)	0.42		789.4	[140]
	0.315	8488.6		[219]
	0.31	6171		[275]
99.3Sn-0.7Cu	0.4371 ± 0.0098		767.6 ± 18.7	[140]
99.3Sn-0.7Cu (1.3 at.% Cu)	0.34	5751		[275]
97Sn-3Cu	0.4295 ± 0.0062		828.0 ± 10.5	[140]
96.5Sn-3.5Ag (3.8 at.% Ag)	0.3795 ± 0.0217		891.2 ± 44.4	[140]
	0.4631 ± 0.0135		717.8 ± 15.5	[140]
	0.37	6612		[275]
96Sn-4Ag	0.4649 ± 0.0063		698.9 ± 7.4	[140]
96.1Sn-3.5Ag-0.4Cu (3.8 at.% Ag -0.7 at.% Cu)	0.35	6433		[275]
95.5Sn-3.8Ag-0.7Cu	0.448	6280		[276]
91Sn-9Zn	0.355	7855.3		[240]
90Sn-10Pb	0.4772 ± 0.0066		702.6 ± 8.1	[140]

wt.% Composition	η_0 (mPa.s)	E_a (J/mol)	E_a/R (K)	Ref.
90Sn-10Ga (84.1 at.% Sn)	0.284	8438.7		[219]
80.3Sn-19.6Ag-0.1Cu (20 at.% Ag -5.7 at.% Cu)	0.37	9295		[275]
75Sn-25Ga (63.8 at.% Sn)	0.255	8189.2		[219]
60Sn-40Pb	0.4791 ± 0.0084		804.8 ± 14.4	[140]
59.9Sn-40.1Ag-0.1Cu (38.8 at.% Ag -8.5 at.% Cu)	0.37	11940		[275]
Sn-Ag-Cu	0.4689 ± 0.0078		725.3 ± 9.5	[140]
Bismuth (Bi)	0.458		775.8	[230]
	0.445		780	[113, 230]
55.5Bi-44.5Pb	0.494		754.1	[113, 230]
	0.425		841.59	[233]
Lead (Pb)	0.455		1069	[113, 230]
	0.543	7889.6		[234]
89.4Pb-10.6Sb (16.75 at.% Sb)	0.530	7495.0		[234]
71.9Pb-28.1Sb (40 at.% Sb)	0.455	7960.9		[234]
53.2Pb-46.8Sb (60 at.% Sb)	0.342	9814.1		[234]
Zinc (Zn)	0.394		1624.2	[123]
87.9Zn-12.1Al (75 at.% Zn)	0.652	7799		[237]
90Zn-10Ga	0.384		1543.7	[123]
75Zn-25Ga	0.379		1399.5	[123]
70Zn-30Al (49 at.% Zn)	0.564	7704		[237]
Antimony (Sb)	0.160	16938.1		[234]
84.1Sb-15.9Pb (90 at.% Sb)	0.167	16090.8		[234]
63.5Mg-31.4Al-5Zn	0.143	14975.1		[238]
60.7Mg-39.3Al (63.2 at.% Mg)	0.157	13046.4		[238]
50.2Mg-49.8Al (52.8 at.% Mg)	0.144	14327.4		[238]
Aluminium (Al)	0.276	12511		[237]
	0.191	14982.4		[238]
66.8Al-33.2Zn (17 at.% Zn)	0.461	8249.5		[237]
63.8Al-36.2Mg (38.6 at.% Mg)	0.131	14710.6		[238]
60.8Al-34.6Mg-4.5Zn	0.114	16928.9		[238]
55Al-43Zn-1.6Si	0.04861	22946.6		[235]
47.4Al-47.7Mg-5Zn	0.093	19124.5		[238]
Calcium (Ca)	1085-1156			[222][(1)]
Lithium (Li)	0.162	4917		[237]

[(1)] Coefficients obtained from data provided

Assael et al. [213, 214] employed the primary viscosity data as a function of the temperature and proposed the following equation form for the viscosity, μ (mPa s), as a function of the absolute temperature, T (K).

$$Log_{10}\left(\mu/\mu_0\right) = -a_1 + a_2/T \qquad (Eq.\ 16)$$

where $\mu_0 = 1mPa.s$, and a_1 is a dimensionless constant and a_2 is a coefficient in K. Table 12 lists the coefficients for temperature-dependent viscosity following Eq. 16.

Table 12: Temperature dependence of Dynamic Viscosity as Eq.16

wt.% Composition	Temp. Range (K)	a_1 (-)	a_2 (K)	Ref.
Gallium	304-800	0.4465	204.03	[214]
Indium	429-1000	0.3621	272.06	[214]
61.9Sn-38.1Pb	450-975	0.2266	280.69	[213]
Bismuth (Bi)	545-1000	0.345	321.4	[231]
55.5Bi-44.5Pb	350-1185	0.3173	346.95	[213]
Lead (Pb)	601-1400	0.295	427.1	[231]
Zinc	695-1100	0.3291	631.12	[214]
Antimony (Sb)	900-1300	0.637	712.5	[231]
88Al-12Si	860-1275	0.8022	658.34	[213]
Silver (Ag)	1235-1500	0.258	1081.8	[231]
Nickel (Ni)	1728-2100	0.505	2108.2	[231]

Other authors present the data for viscosity dependence of temperature according to the following linear equation [223]:

$$ln\left(\mu/\mu_0\right) = b_1/T + b_2 \qquad [mPa\,s] \qquad (Eq.\ 17)$$

Table 13 shows the coefficients for temperature-dependent viscosity following Eq. 17.

Table 13: Temperature dependence of Dynamic Viscosity as Eq.17

wt.% Composition	Temp. Range (K)	b_1 (K)	b_2 (-)	Ref.
99.3Sn-0.7Cu	457-1471	677.5	-0.623	[223]
91.2Sn-8.8Zn	471-845	689.9	-0.762	[223]
57.5Bi-42.5Sn	575-871	797.5	-0.847	[223]
94.7Al-5.3Zn	399-1023	254.9	0.328	[223]
95.8Ag-4.2Sn	493-1474	892.4	-1.145	[223]

The temperature dependence of the viscosity of Bi-Zn liquid alloys measured by Mudry et al. [273] is shown in Fig. 11. Sklyarchuk et al. [277] experimentally obtained the temperature dependence of the viscosity of Bi-Ga liquid alloys measured by Sklyarchuk et al. [277] are shown in Fig. 12.

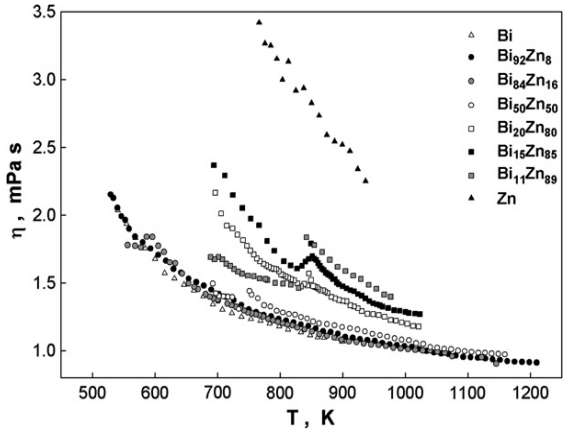

Fig. 11: Viscosity of liquid Bi, Zn and six Bi–Zn melts. Reprinted from [273] with permission from Elsevier

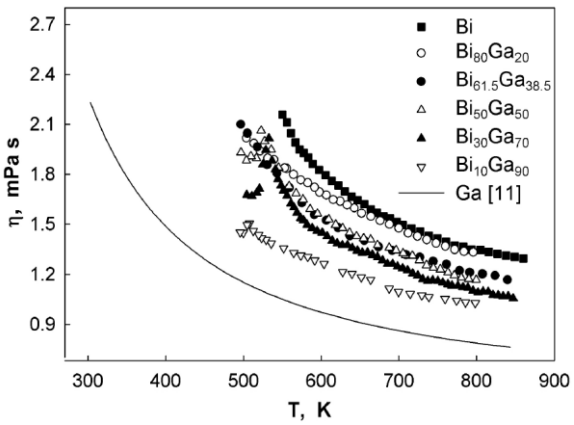

Fig. 12: Viscosities of liquid Bi, Ga and five melts of the Bi-Ga system. [277]

Mitra [222] derived a three-constant equation for the temperature dependence of the coefficient of viscosity (Eq.18) and an equation connecting viscosity, density, and temperature that was found to apply very well for a large number of liquids including molten metals (Eq.19).

$$\mu = \left(A + {}^{B}/_{T} + CT\right)^{3} \qquad \textit{(Eq. 18)}$$

$$\left({}^{\mu}/_{\rho}\right)^{1/3} = a + {}^{b}/_{T} \qquad \textit{(Eq. 19)}$$

where μ is the dynamic viscosity in mP, is the density in g/cm^3, and a and b are constants. Konstantinova et al. [216] calculated the kinematic viscosity of the copper–aluminium melts using the densities of the copper–aluminium melts for different compositions.

Guanbao et al. [278] measured the kinematic viscosity ν of Mg–Al alloys containing up to 14 at.% Al by the method of damped torsional vibrations of a crucible with a melt. The temperature dependences of the kinematic viscosity obtained upon cooling were then approximated by the Arrhenius equation as follows:

$$\nu(T) = \nu_0 exp\left({}^{E_a}/_{RT}\right) \qquad \textit{(Eq. 20)}$$

The coefficients in Arrhenius's equation found for some alloys are given in Table 14.

Table 14: Temperature dependence of Kinematic Viscosity (Eq.20)

wt.% Composition	ν_0 (m²/s)	E_a (J/mol)	Ref.
Magnesium (Mg)	1.07E-7	17300	[278]
95Mg-5Al (4.53 at.% Al)	1.27E-7	14200	[278]
93Mg-7Al (6.35 at.% Al)	1.13E-7	14500	[278]
91Mg-9Al (8.18 at.% Al)	1.37E-7	13100	[278]
89Mg-11Al (10.02 at.% Al)	1.62E-7	9700	[278]
87Mg-13Al (11.86 at.% Al)	2.43E-7	7600	[278]
85Mg-15Al (13.72 at.% Al)	3.41E-7	5300	[278]

Sklyarchuk et al. [279] studied the temperature dependence of thermal conductivity and viscosity for Pb-Sn melts in a wide temperature interval. They found that the experimental data on the

thermal conductivity were in good agreement with the data calculated by electrical conduction. Also, they verified that during the cooling, the viscosity increases by the Arrhenius law.

Table 15 indicates some of the expansion coefficients and dynamic viscosity reported in the literature.

Table 15: Thermal Expansion Coefficients and Dynamic viscosity for some alloys

wt.% Composition	Temp. Range (°C)	Viscosity (mPa s)	α Linear Thermal Exp. Coeff. (s) (1/K)	β Volumetric Thermal Exp. Coeff. (l) (1/K)	Ref.
Gallium (Ga)		1.75		1.2E-4	[192]
		2.04		9.85E-5	[207]
	20		1.80E-5		[217]
52In-48Sn	30(s) 120 (l)		2.874E-5 (s)	2.351E-5 (l)	[182]
49Bi-21In-18Pb-12Sn		1.2 Pa.s*		2.30E-5	[158]
Aluminium	20-660 (s) 660-760 (l)		2.77E-5	0.90E-4	[280]
88Al-12Si ($AlSi_{12}$ at.%)	572-580	2.96	21.60E-6	10 E-6	[78]
	20-579 (Linear) 579-679		1.70E-5	1.30E-5	[280]
			20.5E-6		[88]
$AlSi_{17.5}$ (at.%)	20-548 (Linear) 548-748		1.50E-5	1.10E-4	[280]
80Al-20Si ($AlSi_{20}$ at.%)			17.6E-6		[88]
	576-585				[78]
98.2Bi-1.5Zn-0.3Al (4.5 at.%Zn-2 at.% Al)			8.17E-4		[263]
93.1Bi-6.6Zn-0.3Al (18 at.%Zn-2 at.% Al)			9.75E-4		[263]
87.5Bi-12.1Zn-0.3Al (30.1 at.%Zn-2 at.% Al)			11.94E-4		[263]
99.2Zn-0.8Al (98 at.%Zn-2 at.% Al)			5.85E-4		[263]
56.2Zn-43.2Bi-0.6Al (79 at.%Zn-2 at.% Al)			9.34E-4		[263]

4. Recommendations and Conclusions

This review collected the fundamental thermophysical properties and temperature dependence properties for metallic PCMs in the published literature. The conducted analysis of the literature enables us to conclude the following:

- The set of thermophysical properties found in the published literature for MPCMs is generally not completed, dispersed, conflicted, and subjected to uncertainties. The lack of an MPCM thermophysical properties handbook is a significant barrier in developing potential applications because of the resources needed to characterize the PCM. In summary, there is a definite necessity to generate an "MPCM Handbook" to design, study, and evaluate the MPCMs in LHTES engineering applications.
- The classification by temperature range of the MPCMs, evidenced that metallics materials have been mostly studied in the high-temperature range, mainly for solar energy thermal storage. MPCMs have not been studied thoroughly for the medium and low-temperature range because of their low specific latent heat, high cost and weight, and container corrosion problems.
- Many researchers pointed out as the main disadvantage of MPCMs for LHTES is their elevated weight. However, It could be in part balance with a detailed analysis of the LHTES system, where the

reduction of the storage volume and the simplified design due to the high thermal conductivity can bring significant advantages. Also, recent research trends evaluate the use of composite or hybrid PCMs combining metal and other organic/inorganic materials.

- The most studied MPCMs for medium-temperature applications are non-compliant with Restriction of Hazardous Substances (RoHS) directives and similar international environmental legislation. MPCMs with banned substances (as lead, cadmium) are not recommended for thermal storage applications with potential risk to the environment or health.
- In high-temperature applications, the most severe problem of MPCMs is their chemical compatibility with containers, also applicable for salt hydrate. The study of encapsulations or packaging technologies of MPCMs and their long-term compatibility with the container is a fundamental research topic for developing this technology in practical applications.
- In low-temperature applications, gallium and Ga-based alloys are the dominant metallic materials. Thermal management is the most studied application for these materials. Supercooling and corrosion problems are the main challenges.
- Innovative LHTES systems for metallic PCMs include solid-solid PCM, miscibility gap binary alloys, composite PCM, metal-organic framework, shape-stabilised.

5. Acknowledgements

This project has received funding from the European Union's Horizon 2020 research and innovation program under Marie Sklodowska-Curie grant agreement No. 705944 (THERMOSTALL). Authors thank K. Mahkamov for his help with the funding acquisition. Acknowledgement to Elsevier for granted permission to reproduce the cited figures.

6. References

1. Telkes, M., *Apparatus for Storaging and Releasing Heat*, U.S.P. Office, Editor. 1957: US.
2. Lane, G.A., *Solar Heat Storage: Latent Heat Materials, Volume 1: Background and Scientific Principles*. 1st ed. 1983: CRC Press; 1 edition.
3. Birchenall, C.E.T., M. . *Thermal storage in metals*. in *Sharing the sun: Solar technology in the seventies; Proceedings of the Joint Conference,*. 1976. Winnipeg, Canada, Cape Canaveral, Fla., International Solar Energy Society, 1976,.
4. Telkes, M., *Thermal energy storage in salt hydrates.* Solar Energy Materials, 1980. **2**(4): p. 381-393.
5. Agyenim, F., Hewitt, N., Eames, P., & Smyth, M. , *A review of materials, heat transfer and phase change problem formulation for latent heat thermal energy storage systems (LHTESS).* Renewable and Sustainable Energy Reviews, 2010. **14**(2): p. 615-628.
6. Barber, D.A., *The World Solar Energy Project, ca. 1954.* Grey Room, Inc. and Massachusetts Institute of Technology, 2013. **51**: p. 64-93.
7. Chen, G., et al., *Thermal performance enhancement of micro-grooved aluminum flat plate heat pipes applied in solar collectors.* Renewable Energy, 2020. **146**: p. 2234-2242.
8. Ali, H.M., *Recent advancements in PV cooling and efficiency enhancement integrating phase change materials based systems – A comprehensive review.* Solar Energy, 2020. **197**: p. 163-198.
9. Xu, B., P. Li, and C. Chan, *Application of phase change materials for thermal energy storage in concentrated solar thermal power plants: A review to recent developments.* Applied Energy, 2015. **160**: p. 286-307.
10. Du, K., et al., *A review of the applications of phase change materials in cooling, heating and power generation in different temperature ranges.* Applied Energy, 2018. **220**: p. 242-273.
11. Pielichowska, K. and K. Pielichowski, *Phase change materials for thermal energy storage.* Progress in Materials Science, 2014. **65**: p. 67-123.

12. Huang, Z., et al., *Experimental and numerical study on thermal performance of Wood's alloy/expanded graphite composite phase change material for temperature control of electronic devices.* International Journal of Thermal Sciences, 2019. **135**: p. 375-385.

13. Shi, Y., et al., *Functional Soft Composites As Thermal Protecting Substrates for Wearable Electronics.* Advanced Functional Materials, 2019. **29**(45).

14. Kim, J., J. Oh, and H. Lee, *Review on battery thermal management system for electric vehicles.* Applied Thermal Engineering, 2019. **149**: p. 192-212.

15. Li, D., et al., *Optical and thermal performance of glazing units containing PCM in buildings: A review.* Construction and Building Materials, 2020. **233**.

16. Khadiran, T., et al., *Advanced energy storage materials for building applications and their thermal performance characterization: A review.* Renewable and Sustainable Energy Reviews, 2016. **57**: p. 916-928.

17. Sardari, P.T., et al., *Discharge of a composite metal foam/phase change material to air heat exchanger for a domestic thermal storage unit.* Renewable Energy, 2020. **148**: p. 987-1001.

18. Sharif, M.K.A., et al., *Review of the application of phase change material for heating and domestic hot water systems.* Renewable and Sustainable Energy Reviews, 2015. **42**: p. 557-568.

19. Seddegh, S., et al., *Solar domestic hot water systems using latent heat energy storage medium: A review.* Renewable and Sustainable Energy Reviews, 2015. **49**: p. 517-533.

20. Abdelrazik, A.S., et al., *A review on recent development for the design and packaging of hybrid photovoltaic/thermal (PV/T) solar systems.* Renewable and Sustainable Energy Reviews, 2018. **95**: p. 110-129.

21. Jankowski, N.R. and F.P. McCluskey, *A review of phase change materials for vehicle component thermal buffering* Applied Energy, 2014. **113**: p. 1525-1561.

22. Jaguemont, J., et al., *Phase-change materials (PCM) for automotive applications: A review.* Applied Thermal Engineering, 2018. **132**: p. 308-320.

23. Werner Kraft and M.K. Altstedde, *Use of metallic Phase Change Materials (mPCM) for heat storage in Electric- and Hybrid Vehicles*, in *Hybrid and Electric Vehicles Conference (HEVC 2016), 6th*. 2016: London, UK.

24. Kumar, N., et al., *Review of stability and thermal conductivity enhancements for salt hydrates.* Journal of Energy Storage, 2019. **24**.

25. Lin, Y., et al., *Review on thermal conductivity enhancement, thermal properties and applications of phase change materials in thermal energy storage.* Renewable and Sustainable Energy Reviews, 2018. **82**: p. 2730-2742.

26. Hale, D.V., Hoover, M. J., & ONeill, M. J. , *Phase Change Materials Handbook*. 1971.

27. Birchenall, C.E. and A.F. Riechman, *Heat Storage in Eutectic Alloys.* Metallurgical Transactions A, 1980. **11**(8): p. 1415-1420.

28. Birchenall, C.E., Güceri, S. I., Farkas, D., Labdon, M. B., Nagaswami, N., & Pregger, B. , *Heat Storage in Alloys Transformation (Final Report)*, NASA, Editor. 1981.

29. Farkas, D., & Birchenall, C. E. , *New Eutectic Alloys and Their Heats of Transformation.* Metallurgical Transactions A, 1985. **16**(3): p. 323-328.

30. Gasanaliev, A.M., & Gamataeva, B. Y., *Heat-accumulating properties of melts.* Russian Chemical Reviews, 2000. **69**(2): p. 179-186.

31. Kenisarin, M., & Mahkamov, K. , *Solar energy storage using phase change materials.* Renewable and Sustainable Energy Reviews, 2007. **11**(9): p. 1913-1965.

32. Liu, M., Saman, W., & Bruno, F. , *Review on storage materials and thermal performance enhancement techniques for high temperature phase change thermal storage systems.* Renewable and Sustainable Energy Reviews, 2012. **16**(4): p. 2118-2132.

33. Cárdenas, B., & León, N. , *High temperature latent heat thermal energy storage: Phase change materials, design considerations and performance enhancement techniques.* Renewable and Sustainable Energy Reviews, 2013. **27**: p. 724-737.

34. Li, Y., Cheng, X., *Review on the low melting point alloys for thermal energy storage and heat transfer applications (In Chinese).* Energy Storage Science and Technology, 2013. **Vol.2**(No.3).

35. Peng, M.Y., et al., *Review of solar thermal energy storage materials*, in *8th Asia-Pacific Power and Energy Engineering Conference (APPEEC 2016),*. 2016: Suzhou, China,. p. 141-151.

36. Alva, G., et al., *Thermal energy storage materials and systems for solar energy applications.* Renewable and Sustainable Energy Reviews, 2017. **68**: p. 693-706.

37. Mohamed, S.A., et al., *A review on current status and challenges of inorganic phase change materials for thermal energy storage systems.* Renewable and Sustainable Energy Reviews, 2017. **70**: p. 1072-1089.

38. Zhou, C. and S. Wu, *Medium- and high-temperature latent heat thermal energy storage: Material database, system review, and corrosivity assessment.* International Journal of Energy Research, 2019. **43**(2): p. 621-661.

39. Sharma, A., Tyagi, V. V., Chen, C. R., & Buddhi, D. , *Review on thermal energy storage with phase change materials and applications.* Renewable and Sustainable Energy Reviews, 2009. **13**(2): p. 318-345.

40. Su, W., J. Darkwa, and G. Kokogiannakis, *Review of solid–liquid phase change materials and their encapsulation technologies.* Renewable and Sustainable Energy Reviews, 2015. **48**: p. 373-391.

41. Khan, Z., Z. Khan, and A. Ghafoor, *A review of performance enhancement of PCM based latent heat storage system within the context of materials, thermal stability and compatibility.* Energy Conversion and Management, 2016. **115**: p. 132-158.

42. Ge, H., Li, H., Mei, S., & Liu, J. , *Low melting point liquid metal as a new class of phase change material: An emerging frontier in energy area.* Renewable and Sustainable Energy Reviews, 2013. **21**: p. 331-346.

43. Soares, N., et al., *Review of passive PCM latent heat thermal energy storage systems towards buildings' energy efficiency.* Energy and Buildings, 2013. **59**: p. 82-103.

44. Cabeza, L.F., Castell, A., Barreneche, C. D., De Gracia, A., & Fernández, A. I. , *Materials used as PCM in thermal energy storage in buildings: A review.* Renewable and Sustainable Energy Reviews, 2011. **15**(3): p. 1675-1695.

45. Tatsidjodoung, P., N. Le Pierrès, and L. Luo, *A review of potential materials for thermal energy storage in building applications.* Renewable and Sustainable Energy Reviews, 2013. **18**: p. 327-349.

46. Blanco-Rodríguez, P., et al., *Thermophysical characterization of Mg–51%Zn eutectic metal alloy: A phase change material for thermal energy storage in direct steam generation applications.* Energy, 2014. **72**: p. 414-420.

47. Risueño, E., et al., *Zinc-rich eutectic alloys for high energy density latent heat storage applications.* Journal of Alloys and Compounds, 2017. **705**: p. 714-721.

48. Sugo, H., E. Kisi, and D. Cuskelly, *Miscibility gap alloys with inverse microstructures and high thermal conductivity for high energy density thermal storage applications.* Applied Thermal Engineering, 2013. **51**(1-2): p. 1345-1350.

49. Post, A., et al., *Price estimation for miscibility gap alloy thermal storage systems.* Renewable Energy and Environmental Sustainability, 2017. **2**.

50. Kisi, E., et al., *Miscibility Gap Alloys: A New Thermal Energy Storage Solution*, in *Transition Towards 100% Renewable Energy. Innovative Renewable Energy.* 2018: Springer.

51. Copus, M., et al., *On-sun testing of Miscibility Gap Alloy thermal storage.* Solar Energy, 2019. **177**: p. 657-664.

52. Reed, S., et al., *Extended thermal cycling of miscibility gap alloy high temperature thermal storage materials.* Solar Energy, 2019. **185**: p. 333-340.

53. Cuskelly, D., et al., *Thermal storage for CSP with miscibility gap alloys*, in *SOLARPACES 2018: International Conference on Concentrating Solar Power and Chemical Energy Systems*. 2019.

54. Reed, S. and E. Kisi, *Miscibility gap alloys with a ceramic matrix for thermal energy storage.* SN Applied Sciences, 2020. **2**(12).

55. Whitfield, T.E., et al., *An Investigation of the Miscibility Gap Controlling Phase Formation in Refractory Metal High Entropy Superalloys via the Ti-Nb-Zr Constituent System.* Metals, 2021. **11**(8).

56. Confalonieri, C. and E. Gariboldi, *Al-Sn Miscibility Gap Alloy produced by Power Bed Laser Melting for application as Phase Change Material.* Journal of Alloys and Compounds, 2021. **881**.

57. Chen, X., et al., *Smart integration of carbon quantum dots in metal-organic frameworks for fluorescence-functionalized phase change materials.* Energy Storage Materials, 2019. **18**: p. 349-355.

58. Chen, X., et al., *Metal-Organic Framework-based Phase Change Materials for Thermal Energy Storage.* Cell Reports Physical Science, 2020. **1**(10).

59. Xu, H., et al., *Studies on graphene-based high modulus foams and low melting alloy-based shape stable phase change materials.* Diamond and Related Materials, 2021. **113**.

60. McGillicuddy, R.D., et al., *Metal-Organic Phase-Change Materials for Thermal Energy Storage.* J Am Chem Soc, 2020. **142**(45): p. 19170-19180.

61. Chen, X., et al., *Facile preparation of Metal/Metal-organic frameworks decorated phase change composite materials for thermal energy storage.* Journal of Energy Storage, 2021. **40**.

62. Zhang, G., et al., *Encapsulation of copper-based phase change materials for high temperature thermal energy storage.* Solar Energy Materials and Solar Cells, 2014. **128**: p. 131-137.

63. Nomura, T., et al., *Microencapsulation of metal-based phase change material for high-temperature thermal energy storage.* Sci Rep, 2015. **5**: p. 9117.

64. Fukahori, R., et al., *Macro-encapsulation of metallic phase change material using cylindrical-type ceramic containers for high-temperature thermal energy storage.* Applied Energy, 2016. **170**: p. 324-328.

65. Abraham, A., M. Schoenitz, and E.L. Dreizin, *Energy storage materials with oxide-encapsulated inclusions of low melting metal.* Acta Materialia, 2016. **107**: p. 254-260.

66. Zhang, F., et al., *Encapsulation of metal-based phase change materials using ceramic shells prepared by spouted bed CVD method.* Solar Energy Materials and Solar Cells, 2017. **170**: p. 137-142.

67. Bueno, M., et al., *Modification of asphalt mixtures for cold regions using microencapsulated phase change materials.* Sci Rep, 2019. **9**(1): p. 20342.

68. Kawaguchi, T., et al., *Microencapsulation of Zn-Al alloy as a new phase change material for middle-high-temperature thermal energy storage applications.* Applied Energy, 2020. **276**.

69. Bao, J., et al., *A medium-temperature, metal-based, microencapsulated phase change material with a void for thermal expansion.* Chemical Engineering Journal, 2021. **415**.

70. Ge, H., & Liu, J. , *Phase change effect of low melting point metal for an automatic cooling of USB flash memory.* Frontiers in Energy, 2012. **6**(3): p. 207-209.

71. Kenisarin, M.M., *High-temperature phase change materials for thermal energy storage.* Renewable and Sustainable Energy Reviews, 2010. **14**(3): p. 955-970.

72. Wang, Z., et al., *Aluminum and silicon based phase change materials for high capacity thermal energy storage.* Applied Thermal Engineering, 2015. **89**: p. 204-208.

73. Gokon, N., et al., *Cyclic Properties of Thermal Storage/Discharge for Al-Si Alloy in Vacuum for Solar Thermochemical Fuel Production.* Energy Procedia, 2015. **69**: p. 1759-1769.

74. He, Q., & Zhang, W. , *A study on latent heat storage exchangers with the high-temperature phase-change material.* International journal of energy research, 2001. **25**(4): p. 331-341.

75. Wei, G., et al., *Thermophysical property measurements and thermal energy storage capacity analysis of aluminum alloys.* Solar Energy, 2016. **137**: p. 66-72.

76. Xie, Y., et al., *Study on the thermal storage properties of Al-Si-Cu-Mg alloy.* IOP Conference Series: Earth and Environmental Science, 2017. **61**: p. 012144.

77. Sun, J.Q., Zhang, R. Y., Liu, Z. P., & Lu, G. H., *Thermal reliability test of Al–34%Mg–6%Zn alloy as latent heat storage material and corrosion of metal with respect to thermal cycling.* Energy Conversion and Management, 2007. **48**(2): p. 619-624.

78. Kotzé, J.P., *Thermal energy storage in metallic phase change materials*, in *Faculty of Engineering*. 2014, Stellenbosch University. p. 195.

79. Wang, X., Liu, J., Zhang, Y., Di, H., & Jiang, Y. , *Experimental research on a kind of novel high temperature phase change storage heater.* Energy Conversion and Management, 2006. **47**(15-16): p. 2211-2222.

80. Kotzé, J.P., von Backström, T. W., & Erens, P. J. , *A combined latent thermal energy storage and Steam Generator Concept Using Melallic Phase Change Materials and Metallic Heat Transfer Fluid for Concentrated Solar Power*, in *SolarPACES*. 2011: Granada, Spain.

81. KotzÃŠ, J.P., von BackstrÃ¦m, T. W., & Erens, P. J. , *High Temperature Thermal Energy Storage Utilizing Metallic Phase Change Materials and Metallic Heat Transfer Fluids.* Journal of Solar Energy Engineering, 2013. **135**(3): p. 035001(1-6).

82. Kotzé, J.P., T.W. von Backström, and P.J. Erens, *Simulation and Testing of a Latent Heat Thermal Energy Storage Unit with Metallic Phase Change Material.* Energy Procedia, 2014. **49**: p. 860-869.

83. Sarvghad, M., et al., *Materials compatibility for the next generation of Concentrated Solar Power plants.* Energy Storage Materials, 2018. **14**: p. 179-198.

84. Ma, F. and P. Zhang, *Investigation on the performance of a high-temperature packed bed latent heat thermal energy storage system using Al-Si alloy.* Energy Conversion and Management, 2017. **150**: p. 500-514.

85. Wang, Z., et al., *Thermal reliability of Al-Si eutectic alloy for thermal energy storage.* Materials Research Bulletin, 2017. **95**: p. 300-306.

86. Fukahori, R., et al., *Thermal analysis of Al–Si alloys as high-temperature phase-change material and their corrosion properties with ceramic materials.* Applied Energy, 2016. **163**: p. 1-8.

87. Nomura, T., et al., *Microencapsulated phase change materials with high heat capacity and high cyclic durability for high-temperature thermal energy storage and transportation.* Applied Energy, 2017. **188**: p. 9-18.

88. Lao, X., et al., *High-temperature alloy/honeycomb ceramic composite materials for solar thermal storage applications: Preparation and stability evaluation.* Ceramics International, 2017. **43**(5): p. 4583-4593.

89. Dindi, A., et al., *Compatibility of an Aluminium-Silicon metal alloy-based phase change material with coated stainless-steel containers.* Journal of Energy Storage, 2020. **32**.

90. Sheng, N., et al., *Synthesis of Al-25 wt% Si@Al2O3@Cu microcapsules as phase change materials for high temperature thermal energy storage.* Solar Energy Materials and Solar Cells, 2019. **191**: p. 141-147.

91. Li, Q., et al., *Fabrication and thermal properties investigation of aluminium based composite phase change material for medium and high temperature thermal energy storage.* Solar Energy Materials and Solar Cells, 2020. **211**.

92. Rodríguez-Aseguinolaza, J., et al., *Thermodynamic study of the eutectic Mg49–Zn51 alloy used for thermal energy storage.* Journal of Thermal Analysis and Calorimetry, 2014. **117**(1): p. 93-99.

93. Blanco-Rodríguez, P., et al., *Experiments on a Lab Scale TES Unit using Eutectic Metal Alloy as PCM.* Energy Procedia, 2015. **69**: p. 769-778.

94. Risueño, E., et al., *Mg-Zn-Al Eutectic Alloys as Phase Change Material for Latent Heat Thermal Energy Storage.* Energy Procedia, 2015. **69**: p. 1006-1013.

95. Risueño, E., et al., *Experimental investigation of Mg-Zn-Al metal alloys for latent heat storage application.* Journal of Alloys and Compounds, 2016. **685**: p. 724-732.

96. Echániz, T., et al., *Thermal emissivity spectra and structural phase transitions of the eutectic Mg-51%Zn alloy: A candidate for thermal energy storage.* Journal of Alloys and Compounds, 2016. **684**: p. 62-67.

97. Risueño, E., et al., *Thermal cycling testing of Zn–Mg–Al eutectic metal alloys as potential high-temperature phase change materials for latent heat storage.* Journal of Thermal Analysis and Calorimetry, 2017. **129**(2): p. 885-894.

98. Ma, B., et al., *Fe-shell/Cu-core encapsulated metallic phase change materials prepared by aerodynamic levitation method.* Applied Energy, 2014. **132**: p. 568-574.

99. Gokon, N., T. Yamaguchi, and T. Kodama, *Cyclic thermal storage/discharge performances of a hypereutectic Cu-Si alloy under vacuum for solar thermochemical process.* Energy, 2016. **113**: p. 1099-1108.

100. Fang, D., et al., *Microstructure and thermal characteristics of Mg–Sn alloys as phase change materials for thermal energy storage.* RSC Adv., 2016. **6**(98): p. 96327-96333.

101. Fang, D., et al., *Preparation, microstructure and thermal properties of Mg-Bi alloys as phase change materials for thermal energy storage.* Applied Thermal Engineering, 2016. **92**: p. 187-193.

102. Chen, H., et al., *Microstructure and phase transition kinetics of Mg–Ni–Zn alloy phase change thermal storage materials.* Journal of Alloys and Compounds, 2020. **829**.

103. Gokon, N., et al., *Thermal charge/discharge performance of iron–germanium alloys as phase change materials for solar latent heat storage at high temperatures.* Journal of Energy Storage, 2020. **30**.

104. Wei, H., et al., *Development of phase change materials using hydrolyzed Al-Bi composite powder for solar energy storage.* Chemical Engineering Journal, 2021. **421**.

105. Rawson, A.J., et al., *Selection of compatible metallic phase change materials and containers for thermal storage applications.* Journal of Energy Storage, 2020. **32**.

106. Nishioka, K., Suura, N., Ohno, K. I., Maeda, T., & Shimizu, M. , *Development of Fe base phase change materials for high temperature using solid–solid transformation.* . ISIJ international, 2010. **50**(9): p. 1240-1244.

107. Reed, S., H. Sugo, and E. Kisi, *High temperature thermal storage materials with high energy density and conductivity.* Solar Energy, 2018. **163**: p. 307-314.

108. Confalonieri, C., A.T. Grimaldi, and E. Gariboldi, *Ball-milled Al–Sn alloy as composite Phase Change Material.* Materials Today Energy, 2020. **17**.

109. Confalonieri, C., M. Perrin, and E. Gariboldi, *Combined powder metallurgy routes to improve thermal and mechanical response of Al–Sn composite phase change materials.* Transactions of Nonferrous Metals Society of China, 2020. **30**(12): p. 3226-3239.

110. Confalonieri, C., P. Bassani, and E. Gariboldi, *Microstructural and thermal response evolution of metallic form-stable phase change materials produced from ball-milled powders.* Journal of Thermal Analysis and Calorimetry, 2020. **142**: p. 85-96.

111. Navarrete, N., et al., *Thermal energy storage of molten salt –based nanofluid containing nano-encapsulated metal alloy phase change materials.* Energy, 2019. **167**: p. 912-920.

112. Corporation, I. *Indium Corporation E List of Alloys.* 2016; 20:[Available from: www.indium.com.

113. Fazio, C., Sobolev, V. P., Aerts, A., Gavrilov, S., Lambrinou, K., Schuurmans, P., ... & Gosse, S. , *Handbook on Lead-bismuth Eutectic Alloy and Lead Properties, Materials Compatibility, Thermal-hydraulics and Technologies*. No. NEA--7268 ed. Organisation for Economic Co-Operation and Development., ed. N. Science. 2015.

114. Hoshi, A., Mills, D. R., Bittar, A., & Saitoh, T. S. , *Screening of high melting point phase change materials (PCM) in solar thermal concentrating technology based on CLFR.* Solar Energy, 2005. **79**(3): p. 332-339.

115. Singh, S.P., B.K. Deb Barman, and P. Kumar, *Cu-Bi alloys with high volume fraction of Bi: A material potentially suitable for thermal surge protection and energy storage.* Materials Science and Engineering: A, 2016. **677**: p. 140-152.

116. Fernández, A.I., et al., *Considerations for the use of metal alloys as phase change materials for high temperature applications.* Solar Energy Materials and Solar Cells, 2017. **171**: p. 275-281.

117. Gómez-Acebo, T., Martín, J. M., Castro, F., & Lardizabal, P. M. , *Systematic search of low melting point alloys in the Al-Cu-Mg-Zn system*, in *European Conference on Powder Metallurgy Euro*. 2003: Valencia (Spain).

118. Nieto-Maestre, J., et al., *Novel metallic alloys as phase change materials for heat storage in direct steam generation applications.* 2016. **1734**: p. 050032.

119. Adinberg, R., Zvegilsky, D., & Epstein, M. , *Heat transfer efficient thermal energy storage for steam generation.* Energy Conversion and Management, 2010. **51**(1): p. 9-15.

120. Saatçi, B., Maraşlı, N., & Gündüz, M. , *Thermal conductivities of solid and liquid phases in Pb–Cd and Sn–Zn binary eutectic alloys.* Thermochimica Acta, 2007. **454**(2): p. 128-134.

121. Fan Xiaoming, et al., *Thermal cycling stability of Mg-25Al-15Zn-14Cu PCM.* Journal of Wuhan University of Technology-Mater. Sci. Ed., 2016. **31**(6): p. 1363-1367.

122. Khare, S., Dell'Amico, M., Knight, C., & McGarry, S. , *Selection of materials for high temperature latent heat energy storage.* Solar Energy Materials and Solar Cells, 2012. **107**: p. 20-27.

123. Gancarz, T., *The physicochemical properties of liquid Ga-Zn alloys.* Fluid Phase Equilibria, 2017. **442**: p. 119-124.

124. Sun, Z., et al., *Thermal Properties and the Prospects of Thermal Energy Storage of Mg-25%Cu-15%Zn Eutectic Alloy as Phase Change Material.* Materials (Basel), 2021. **14**(12).

125. Cui, F., Yuan, Y., Zhao, J., Cao, X., Sun, L. and S. Liangliang, *Influence of Cu content on thermal characteristics of high-temperature phase change material Al-Cu alloy.* CIESC Journal, 2017.

126. Morando, C., et al., *Fluidity on Metallic Eutectic Alloys.* Procedia Materials Science, 2015. **8**: p. 959-967.

127. Gil, A., Medrano, M., Martorell, I., Lázaro, A., Dolado, P., Zalba, B., & Cabeza, L. F., *State of the art on high temperature thermal energy storage for power generation. Part 1—Concepts, materials and modellization.* Renewable and Sustainable Energy Reviews, 2010. **14**(1): p. 31-55.

128. Andraka, C.E., et al., *Metallic Phase Change Material Thermal Storage for Dish Stirling.* Energy Procedia, 2015. **69**: p. 726-736.

129. Zhou, K., et al., *Composition, Microstructure, Phase Constitution and Fundamental Physicochemical Properties of Low-Melting-Point Multi-Component Eutectic Alloys.* Journal of Materials Science & Technology, 2017. **33**(2): p. 131-154.

130. Mei, Z., H.A. Holder, and H.A.V. Plas, *Low-Temperature Solders*, in *Hewlett-Packard Journal*. 1996.

131. Corporation, I., *How to Use Fusible Alloys*. INDIUM Corporation.

132. Gurrum, S.P., Joshi, Y. K., & Kim, J. , *Thermal Management of High Temperature Pulsed Electronics Using Metallic Phase Change Materials.* Numerical Heat Transfer, Part A: Applications, 2002. **42**(8): p. 777-790.

133. Yoo, D.W., & Joshi, Y. K. , *Energy Efficient Thermal Management of Electronic Components Using Solid–Liquid Phase Change Materials.* IEEE Transactions on Device and Materials Reliability, 2004. **4**(4): p. 641-649.

134. *The Restriction of the Use of Certain Hazardous Substances in Electrical and Electronic Equipment Regulations 2012*. 2012.

135. Union, O.J.o.t.E., *DIRECTIVE 2011/65/EU OF THE EUROPEAN PARLIAMENT AND OF THE COUNCIL of 8 June 2011 on the restriction of the use of certain hazardous substances in electrical and electronic equipment*. 2011. p. L174:54: 88-110.

136. Abtew, M. and G. Selvaduray, *Lead-Free Solders in Microelectronics.* Master Science and Engineering, 2000. **27**: p. 95-141.

137. Suganuma, K., *Advances in lead-free electronics soldering.* Current Opinion in Solid State and Materials Science, 2001. **5**(1): p. 55–64.

138. Mavoori, H., Ramirez, A. G., & Jin, S. , *Lead-Free Universal Solders for Optical and Electronic Devices.* Journal of electronic materials, 2002. **31**(11): p. 1160-1162.

139. Siewert, T., Liu, S., Smith, D. R., & Madeni, J. C. , *Properties of lead-free solders. Database for solder properties with emphasis on new lead-free solders, Release, 4.* 2002, NIST.

140. Mhiaoui, S., *Physical properties of lead free solders in liquid and solid state*. 2007, Technischen Universität Chemnitz.

141. Handwerker, C., et al., *Chapter 2: Fundamental Properties of Pb-Free Solder Alloys*, in *Lead-Free Soldering*. 2007.

142. El-Daly, A.A., Swilem, Y., Makled, M. H., El-Shaarawy, M. G., & Abdraboh, A. M. , *Thermal and mechanical properties of Sn–Zn–Bi lead-free solder alloys.* Journal of Alloys and Compounds, 2009. **484**(1-2): p. 134-142.

143. Palcut, M., Sopousek, J., Trnková, L., Hodulova, E., Szewczyková, B., Ozvold, M., ... & Janovec, J. , *Thermal analysis of selected tin-based lead-free solder alloys.* Kovove Mater., 2009. **47**: p. 43-50.

144. Hu, y., Cao, F., Li, F., Ni, G.,Cui,X., *Rearch Progress on Lead-Free solders.* Rev. Adv. Mater. Sci., 2011. **29**: p. 150-155.

145. El-Daly, A.A., et al., *Design of lead-free candidate alloys for low-temperature soldering applications based on the hypoeutectic Sn–6.5Zn alloy.* Materials & Design (1980-2015), 2014. **56**: p. 594-603.

146. Shu, Y., et al., *Synthesis and thermal properties of low melting temperature tin/indium (Sn/In) lead-free nanosolders and their melting behavior in a vapor flux.* Journal of Alloys and Compounds, 2015. **626**: p. 391-400.

147. El-Daly, A.A., A.M. El-Taher, and S. Gouda, *Development of new multicomponent Sn–Ag–Cu–Bi lead-free solders for low-cost commercial electronic assembly.* Journal of Alloys and Compounds, 2015. **627**: p. 268-275.

148. Gąsior, W., Moser, Z., Dębski, A., & Siewert, T. , *Integration of the NIST and SURDAT Databases on Physical Properties of Lead-Free Solder Alloys.* International Journal of Thermophysics, 2010. **31**(3): p. 502-512.

149. Zhou, J., Sun, Y., & Xue, F. , *Properties of low melting point Sn–Zn–Bi solders.* Journal of Alloys and Compounds, 2005. **397**(1-2): p. 260-264.

150. Lin, D.C., Srivatsan, T. S., Wang, G. X., & Kovacevic, R. , *Microstructural development in a rapidly cooled eutectic Sn–3.5% Ag solder reinforced with copper powder.* Powder Technology, 2006. **166**(1): p. 38-46.

151. Morando, C., et al., *Thermal properties of Sn-based solder alloys.* Journal of Materials Science: Materials in Electronics, 2014. **25**(8): p. 3440-3447.

152. Moser, Z., et al., *SURDAT: DATABASE OF LEAD - FREE SOLDERING MATERIALS*. 200, Kraków.

153. Schmetterer, M.C., Mikula, A., Ipser, H., *DATABASE FOR PROPERTIES OF LEAD-FREE SOLDER ALLOYS*, in *COST351*. 2006.

154. Fan, L.-W., et al., *Transient performance of a thermal energy storage-based heat sink using a liquid metal as the phase change material.* Applied Thermal Engineering, 2016. **109**: p. 746-750.

155. Huang, Z., et al., *Preparation and thermal property analysis of Wood's alloy/expanded graphite composite as highly conductive form-stable phase change material for electronic thermal management.* Applied Thermal Engineering, 2017. **122**: p. 322-329.

156. Gao, J.-Y., et al., *Numerical investigation on integrated thermal management via liquid convection and phase change in packed bed of spherical low melting point metal macrocapsules.* International Journal of Heat and Mass Transfer, 2020. **150**.

157. Yang, T., et al., *A composite phase change material thermal buffer based on porous metal foam and low-melting-temperature metal alloy.* Applied Physics Letters, 2020. **116**(7).

158. Zhao, L., et al., *The passive thermal management system for electronic device using low-melting-point alloy as phase change material.* Applied Thermal Engineering, 2017. **125**: p. 317-327.

159. Huang, P., et al., *Numerical investigation of a dual-PCM heat sink using low melting point alloy and paraffin.* Applied Thermal Engineering, 2021. **189**.

160. Mawire, A., et al., *Performance comparison of two metallic eutectic solder based medium-temperature domestic thermal energy storage systems.* Energy, 2020. **194**.

161. Mawire, A., et al., *Performance of a medium temperature eutectic solder packed bed latent heat storage system for domestic applications.* Journal of Energy Storage, 2020. **28**.

162. Zhong, Y., Guo, Q., Li, S., Shi, J., & Liu, L. , *Thermal and mechanical properties of graphite foam/Wood's alloy composite for thermal energy storage.* Carbon, 2010. **48**(5): p. 1689-1692.

163. Zhong, Y., Guo, Q., Li, L., Wang, X., Song, J., Xiao, K., & Huang, F., *Heat transfer improvement of Wood's alloy using compressed expanded natural graphite for thermal energy storage.* Solar Energy Materials and Solar Cells, 2012. **100**: p. 263-267.

164. ASTM, *ASTM B 774 – 00: Low Melting Point Alloys (Standard)*. 2000.

165. Krishnan, S., Garimella, S. V., & Kang, S. S. , *A novel hybrid heat sink using phase change materials for transient thermal management of electronics.* IEEE Transactions on Components and Packaging Technologies, 2005. **28**(2): p. 281-289.

166. Fukuoka, Y., Matsumoto, E., & Ishizuka, M. , *New Package Cooling Technology Using Low Melting Point Alloys.* Microelectronics International, 1987. **4**(3): p. 13-18.

167. Fukuoka, Y., & Ishizuka, M. , *Thermal Analysis of a New High Density Package Cooling Tech using low melting point alloys.* Japanese Journal of Applied Physics, 1991. **30**(6): p. 1313-1319.

168. Yang, X.-H., et al., *Evaluation and optimization of low melting point metal PCM heat sink against ultra-high thermal shock.* Applied Thermal Engineering, 2017. **119**: p. 34-41.

169. Shamberger, P.J., Y. Mizuno, and A.A. Talapatra, *Mixing and electronic entropy contributions to thermal energy storage in low melting point alloys.* Journal of Applied Physics, 2017. **122**(2): p. 025105.

170. Zhang, Q. and J. Liu, *Nano liquid metal as an emerging functional material in energy management, conversion and storage.* Nano Energy, 2013. **2**(5): p. 863-872.

171. Pacio, J., et al., *Thermodynamic evaluation of liquid metals as heat transfer fluids in concentrated solar power plants.* Applied Thermal Engineering, 2013. **60**(1-2): p. 295-302.

172. Pacio, J. and T. Wetzel, *Assessment of liquid metal technology status and research paths for their use as efficient heat transfer fluids in solar central receiver systems.* Solar Energy, 2013. **93**: p. 11-22.

173. Standards, B., *Soft solder alloys — Chemical compositions and forms (ISO 9453:2014)*. 2014.

174. Bilek, J., Atkinson, J. K., & Wakeham, W. A. , *Thermal Conductivity of Molten Lead-Free Solders.* International Journal of Thermophysics, 2006. **27**(1): p. 92-102.

175. Coen, G., Van den Bosch, J., Almazouzi, A., & Degrieck, J. , *Investigation of the effect of lead–bismuth eutectic on the fracture properties of T91 and 316L.* Journal of Nuclear Materials, 2010. **398**(1-3): p. 122-128.

176. Van den Bosch, J., Hosemann, P., Almazouzi, A., & Maloy, S. A. , *Liquid metal embrittlement of silicon enriched steel for nuclear applications.* Journal of Nuclear Materials, 2010. **398**(1-3): p. 116-121.

177. Lim, J., Nam, H. O., Hwang, I. S., & Kim, J. H. , *A study of early corrosion behaviors of FeCrAl alloys in liquid lead–bismuth eutectic environments.* Journal of Nuclear Materials, 2010. **407**(3): p. 205-210.

178. Cho, J.H., Batta, A., Casamassima, V., Cheng, X., Choi, Y. J., Hwang, I. S., ... & Kuznetsov, V. , *Benchmarking of thermal hydraulic loop models for Lead-Alloy Cooled Advanced Nuclear Energy*

System (LACANES), phase-I: Isothermal steady state forced convection. Journal of Nuclear Materials, 2011. **415**(3): p. 404-414.

179. Ilincˇev, G., *Research results on the corrosion effects of liquid heavy metals Pb, Bi and Pb–Bi on structural materials with and without corrosion inhibitors.* Nuclear Engineering and Design, 2002. **217**: p. 167-177.

180. Meydaneri, F., B. Saat, and M. Ozdemir, *Thermal, electrical, microstructure and microhardness properties of the eutectic Sn-3.5wt.%Ag alloy.* 2013.

181. Yang, X.-H., et al., *Experimental and numerical investigation of low melting point metal based PCM heat sink with internal fins.* International Communications in Heat and Mass Transfer, 2017. **87**: p. 118-124.

182. Goodfield, D., A. Mawire, and A.B. Shobo, *Investigation of In–48Sn as a phase change material candidate for thermal storage applications.* Renewable Energy and Environmental Sustainability, 2017. **2**: p. 20.

183. Venkitaraj, K.P. and S. Suresh, *Experimental study on thermal and chemical stability of pentaerythritol blended with low melting alloy as possible PCM for latent heat storage.* Experimental Thermal and Fluid Science, 2017. **88**: p. 73-87.

184. Yang, E., et al., *Thermal Performance of Low-Melting-Temperature Alloy Thermal Interface Materials.* Acta Metallurgica Sinica (English Letters), 2014. **27**(2): p. 290-294.

185. Yang, Y.S., & Tsao, C. Y. , *Viscosity and structure variations of Al–Si alloy in the semi-solid state.* Journal of Materials Science & Technology, 1997. **32**: p. 2087—2092.

186. Manasijević, D., et al., *Thermal characterization of the In–Sn–Zn eutectic alloy.* Metallurgical and Materials Engineering, 2020. **25**(04): p. 325-334.

187. Dutchak, Y.I., Osipenko, V. P., & Panasyuk, P. V. , *Thermal conductivity of Sn-Bi alloys in the solid and liquid states.* Soviet Physics Journal, 1968. **11**(10): p. 145-147.

188. Çadırlı, E., Şahin, M., Kayalı, R., Arı, M., & Durmuş, S. , *Dependence of electrical and thermal conductivity on temperature in directionally solidified Sn–3.5 wt% Ag eutectic alloy.* Journal of Materials Science: Materials in Electronics, 2011. **22**(11): p. 1709-1714.

189. Meydaneri, F. and B. Saatçi, *Thermal, Electrical, Microstructure and Microhardness Properties of the Eutectic Magnesium–Tin.* Arabian Journal for Science and Engineering, 2014. **39**(7): p. 5815-5824.

190. Ocak, Y., Aksöz, S., Maraşlı, N., & Keşlioğlu, K. , *Thermal conductivity and interfacial energies of solid Sn solution in the Sn–Ag–In ternary alloy.* Chemical Physics Letters, 2010. **496**(4-6): p. 263-269.

191. Nagai, H., Mamiya, M., Castillo, M., & Okutani, T. , *Development of Hot-Disk Sensor for Molten Metal, and the Thermal Conductivity Measurement of Molten Bismuth and Tin using Hot-Disk Method.* Japanese Journal of Applied Physics, 2006. **45**(8A): p. 6455-6461.

192. Yang, X.-H., S.-C. Tan, and J. Liu, *Numerical investigation of the phase change process of low melting point metal.* International Journal of Heat and Mass Transfer, 2016. **100**: p. 899-907.

193. Arshad, A., et al., *Experimental investigation of PCM based round pin-fin heat sinks for thermal management of electronics: Effect of pin-fin diameter.* International Journal of Heat and Mass Transfer, 2018. **117**: p. 861-872.

194. Yang, X.-H., et al., *Finned heat pipe assisted low melting point metal PCM heat sink against extremely high power thermal shock.* Energy Conversion and Management, 2018. **160**: p. 467-476.

195. Al Omari, S.A.B., A.M. Ghazal, and E. Elnajjar, *A new approach using un-encapsulated discrete PCM chunks to augment the applicability of solid gallium as phase change material in thermal management applications.* Energy Conversion and Management, 2018. **158**: p. 133-146.

196. Zhang, X.-D., et al., *Comparison on Enhanced Phase Change Heat Transfer of Low Melting Point Metal Melting Using Different Heating Methods.* Journal of Enhanced Heat Transfer, 2019. **26**(2): p. 179-194.

197. Salyan, S., et al., *Liquid Metal Gallium in Metal Inserts for Solar Thermal Energy Storage: A Novel Heat Transfer Enhancement Technique.* Solar Energy Materials and Solar Cells, 2020. **208**.

198. Salyan, S. and S. Suresh, *Liquid metal gallium laden organic phase change material for energy storage: An experimental study.* International Journal of Hydrogen Energy, 2018. **43**(4): p. 2469-2483.

199. Kondo, M., M. Ishii, and T. Muroga, *Corrosion of steels in molten gallium (Ga), tin (Sn) and tin lithium alloy (Sn–20Li).* Fusion Engineering and Design, 2015. **98-99**: p. 2003-2008.

200. Shin, S.H., Kim, J. J., Jung, J. A., Choi, K. J., Bang, I. C., & Kim, J. H. , *A study on corrosion behavior of austenitic stainless steel in liquid metals at high temperature.* Journal of Nuclear Materials, 2012. **422**(1-3): p. 92-102.

201. Shin, Y.-H., et al., *Advanced passive design of small modular reactor cooled by heavy liquid metal natural circulation.* Progress in Nuclear Energy, 2015. **83**: p. 433-442.

202. Dai, D., Zhou, Y., & Liu, J. , *Liquid metal based thermoelectric generation system for waste heat recovery.* Renewable Energy, 2011. **36**(12): p. 3530-3536.

203. Malakooti, M.H., et al., *Liquid Metal Supercooling for Low-Temperature Thermoelectric Wearables.* Advanced Functional Materials, 2019. **29**(45).

204. Plevachuk, Y., et al., *Thermophysical Properties of the Liquid Ga–In–Sn Eutectic Alloy.* Journal of Chemical & Engineering Data, 2014. **59**(3): p. 757-763.

205. Deng, Y.G., & Liu, J. , *Corrosion development between liquid gallium and four typical metal substrates used in chip cooling device.* Applied Physics A, 2009. **95**(3): p. 907-915.

206. Zhang, C., et al., *Study on the nucleating agents for gallium to reduce its supercooling.* International Journal of Heat and Mass Transfer, 2020. **148**.

207. Fukuyama, H., Yoshimura, T., Yasuda, H., & Ohta, H. , *Thermal Conductivity Measurements of Liquid Mercury and Gallium by a Transient Hot-Wire Method in a Static Magnetic Field.* International Journal of Thermophysics, 2006. **27**(6): p. 1760-1777.

208. Svein Stolen, F.G., *Critical Assesment of the enthalpy of fusion of metals used as moderate standards at moderate high temperature.* Thermochimical Acta, 1999.

209. Kenisarin, M.M., *Thermophysical properties of some organic phase change materials for latent heat storage. A review.* Solar Energy, 2014. **107**: p. 553-575.

210. Pan, A., J. Wang, and X. Zhang, *Prediction of Melting Temperature and Latent Heat for Low-melting Metal PCMs.* Rare Metal Materials and Engineering, 2016. **45**(4): p. 874-880.

211. Thresh, H.R., & Crawley, A. F. , *The viscosities of lead, tin, and Pb-Sn alloys.* Metallurgical Transactions, 1970. **1**(6): p. 1531-1535.

212. Valencia, J.J.Q., P.N., *Thermophysical Properties.* ASM Handbook, 2008. **Volume 15: Casting**: p. p 468-481.

213. Assael, M.J., Mihailidou, E. K., Brillo, J., Stankus, S. V., Wu, J. T., & Wakeham, W. A. , *Reference Correlation for the Density and Viscosity of Eutectic Liquid Alloys Al+Si, Pb+Bi, and Pb+Sn.* Journal of Physical and Chemical Reference Data, 2012. **41**(3): p. 033103 (1-9).

214. Assael, M.J., Armyra, I. J., Brillo, J., Stankus, S. V., Wu, J., & Wakeham, W. A. , *Reference Data for the Density and Viscosity of Liquid Cadmium, Cobalt, Gallium, Indium, Mercury, Silicon, Thallium, and Zinc.* Journal of Physical and Chemical Reference Data, 2012. **41**(3): p. 033101 (1-16).

215. Khairulin, R.A., Stankus, S. V., Abdullaev, R. N., & Sklyarchuk, V. M. , *The density and interdiffusion coefficients of bismuth-tin melts of eutectic and near-eutectic composition.* High Temperature, 2010. **48**(2): p. 188–191.

216. Konstantinova, N.Y., et al., *Viscosity of aluminum–copper melts.* Russian Metallurgy (Metally), 2016. **2016**(2): p. 144-149.

217. Prokhorenko, V.Y., Roshchupkin, V. V., Pokrasin, M. A., Prokhorenko, S. V., & Kotov, V. V., *Liquid Gallium. Potential Uses as a Heat-Transfer Agent.* High Temperature, 2000. **38**(6): p. 954–968.

218. Chentsov, V.P., Shevchenko, V. G., Mozgovoi, A. G., & Pokrasin, M. A. , *Density and surface tension of heavy liquid-metal coolants: Gallium and indium.* Inorganic Materials: Applied Research, 2011. **2**(5): p. 468-473.

219. Gancarz, T., *Density, surface tension and viscosity of Ga-Sn alloys.* Journal of Molecular Liquids, 2017. **241**: p. 231-236.

220. Dobosz, A., et al., *Thermophysical properties of the liquid Ga–Sn–Zn eutectic alloy.* Fluid Phase Equilibria, 2018. **465**: p. 1-9.

221. Stankus, S.V., et al., *Studies of the thermophysical properties of substances and materials at the Novosibirsk Scientific Center of the Siberian Branch of the Russian Academy of Sciences, 2002–2012.* High Temperature, 2013. **51**(5): p. 695-711.

222. Mitra, S.S., *Viscosity and density of liquid metals.* Physica, 1958. **24**(1-5): p. 155-156.

223. Dobosz, A., & Gancarz, T. , *Reference Data for the Density, Viscosity, and Surface Tension of Liquid Al–Zn, Ag–Sn, Bi–Sn, Cu–Sn, and Sn–Zn Eutectic Alloys.* Journal of Physical and Chemical Reference Data 2018. **47**(1).

224. Fima, P., *Surface tension and density of liquid Sn–Ag alloys.* Applied Surface Science, 2011. **257**(8): p. 3265-3268.

225. Fima, P., *Surface tension and density of liquid Sn–Cu alloys.* Applied Surface Science, 2010. **257**(2): p. 468-471.

226. Yagodin, D., Sidorov, V., Janickovic, D., & Svec, P. , *Density studies of liquid alloys SnAg and SnZn with near eutectic compositions.* Journal of Non-Crystalline Solids, 2012. **358**(21): p. 2935-2937.

227. Fima, P., *Surface tension and density of liquid Sn–Ag–Cu alloys.* International Journal of Materials Research, 2012. **103**(12): p. 1455-1461.

228. Guo, Z., Hindler, M., Yuan, W., & Mikula, A. , *Density and surface tension of liquid Bi–Cu–Sn alloys.* Monatshefte für Chemie - Chemical Monthly, 2012. **143**(12): p. 1617-1622.

229. Plevachuk, Y., Sklyarchuk, V., Gerbeth, G., Eckert, S., & Novakovic, R., *Surface tension and density of liquid Bi–Pb, Bi–Sn and Bi–Pb–Sn eutectic alloys.* Surface Science, 2011. **605**(11-12): p. 1034-1042.

230. OECD/NEA Nuclear Science Committee. Working Party on Scientific Issues of the Fuel Cycle, W.G.o.L.B.E., *Handbook on Lead–Bismuth Eutectic Alloy and Lead Properties, Materials Compatibility, Thermal-Hydraulics and Technologies.* . 2007: Nuclear Energy Agency Organisation for Economic Co-operation and Development.

231. Assael, M.J., Kalyva, A. E., Antonia, K. D., Banish, R. M., Egry, I., Wu, J., ... & Wakeham, W. A. , *Reference data for the density and viscosity of liquid antimony, bismuth, lead, nickel and silver.* High Temperatures--High Pressures, 2012. **41**(3): p. 161-184.

232. Stankus, S.V., Khairulin, R. A., Mozgovoi, A. G., Roshchupkin, V. V., & Pokrasin, M. A. , *The density of a liquid Pb-Bi alloy of eutectic composition at temperatures up to 700 K.* High Temperature 2004. **42**: p. 999–1002.

233. Filippov, V.V., et al., *Density, viscosity, ultrasound velocity, and electrical resistivity of the eutectic lead–bismuth melt.* Russian Metallurgy (Metally), 2016. **2016**(8): p. 705-708.

234. Gancarz, T. and W. Gasior, *Density, Surface Tension, and Viscosity of Liquid Pb–Sb Alloys.* Journal of Chemical & Engineering Data, 2018. **63**(5): p. 1471-1479.

235. Nunes, V.M.B., et al., *Viscosity of Industrially Important Zn–Al Alloys Part II: Alloys with Higher Contents of Al and Si.* International Journal of Thermophysics, 2018. **39**(5).

236. Hopkins, M.R., & Toye, T. C. . *The Determination of the Viscosity of Molten Metals*. in *Proceedings of the Physical Society*. 1950.

237. Trybula, M.E., T. Gancarz, and W. Gąsior, *Density, surface tension and viscosity of liquid binary Al-Zn and ternary Al-Li-Zn alloys.* Fluid Phase Equilibria, 2016. **421**: p. 39-48.

238. Gancarz, T., et al., *Physicochemical properties of Al, Al-Mg and Al-Mg-Zn alloys.* Journal of Molecular Liquids, 2018. **249**: p. 470-476.

239. Crawley, A.F., *Densities and viscosities of some liquid alloys of zinc and cadmium.* Metallurgical Transactions 1972. **3**.

240. Gancarz, T., Pstruś, J., Gąsior, W., & Henein, H. , *Physicochemical Properties of Sn-Zn and SAC + Bi Alloys.* Journal of Electronic Materials, 2012. **42**(2): p. 288-293.

241. Khairulin, R.A., & Stankus, S. V. , *Determination of the density of Pb-Sn melts and segregation phenomena on their crystallization.* Journal of Engineering Thermophysics, 2007. **16**(3): p. 188-191.

242. Khairulin, R.A., Kosheleva, A. S., & Stankus, S. V. , *Thermal properties of liquid alloys of magnesium-lead system.* Thermophysics and Aeromechanics, 2007. **14**(1): p. 75-80.

243. Li, Z., C. Confalonieri, and E. Gariboldi, *Numerical and Experimental Evaluation of Thermal Conductivity: An Application to Al-Sn Alloys.* Metals, 2021. **11**(4).

244. Duggin, M.J., *The thermal conductivity of liquid gallium.* Physics Letters A, 1969. **29**(8): p. 470-471.

245. Pashaev, B.P., Palchaev, D. K., Pashuk, E. G., & Revelis, V. G. , *Thermophysical properties of polyvalent metals and their alloys in the solid and liquid states.* Journal of engineering physics 1980. **38**(4): p. 358-363.

246. Assael, M.J., et al., *Reference correlations for the thermal conductivity of liquid copper, gallium, indium, iron, lead, nickel and tin.* High Temperatures-High Pressures, 2017. **46**: p. 391–416.

247. Savchenko, I.V., Stankus, S. V., & Agazhanov, A. S. , *Heat transfer coefficients of liquid indium in the temperature range 470−1275 K.* Thermophysics and Aeromechanics, 2010. **17**(1): p. 121-125.

248. Stankus, S.V., Savchenko, I. V., & Agazhanov, A. S. , *Thermal Conductivity and Thermal Diffusivity of Liquid Indium–Tin Alloys.* International Journal of Thermophysics, 2012. **33**(5): p. 774-782.

249. Aksöz, N., Öztürk, E., Bayram, Ü., Aksöz, S., Kervan, S., Ülgen, A., & Maraşlı, N. , *Thermal Conductivity Variation with Temperature for Lead-Free Ternary Eutectic Solders.* Journal of Electronic Materials, 2013. **42**(12): p. 3573-3581.

250. Savchenko, I.V.E., Stankus, S. V., & Agadjanov, A. S. , *Measurement of liquid tin heat transfer coefficients within the temperature range of 506–1170 K.* High Temperature, 2011. **49**(4): p. 506-511.

251. Demir, M., et al., *The Measurement of Thermal Conductivity Variation with Temperature for Sn-Based Lead-Free Binary Solders.* Metallurgical and Materials Transactions B, 2014. **45**(5): p. 1739-1749.

252. Meydaneri, F., Gündüz, M., Özdemir, M., & Saatçi, B., *Determination of thermal conductivities of solid and liquid phases for rich-Sn compositions of Sn-Mg alloy.* Metals and Materials International, 2012. **18**(1): p. 77-85.

253. Meydaneri Tezel, F., et al., *Structural and thermo-electrical properties of Sn–Al alloys.* Applied Physics A, 2016. **122**(10).

254. Kaygısız, Y., Ocak, Y., Aksöz, S., Maraşlı, N., Keşlioğlu, K., Çadırlı, E., & Kaya, H. , *Thermal conductivity and interfacial energies of solid Sn in the Sn–Cu alloy.* Chemical Physics Letters, 2010. **484**(4-6): p. 219-224.

255. Meydaneri, F., Saatçi, B., & Özdemir, M. , *Thermal conductivities of solid and liquid phases for pure Al, pure Sn and their binary alloys.* Fluid Phase Equilibria, 2010. **298**(1): p. 97-105.

256. Ocak, Y., Aksöz, S., Maraşlı, N., & Çadırlı, E. , *Dependency of thermal and electrical conductivity on temperature and composition of Sn in Pb–Sn alloys.* Fluid Phase Equilibria, 2010. **295**(1): p. 60-67.

257. Meydaneri, F., Saatçi, B., Gündüz, M., & Özdemir, M. , *Determination of thermal conductivities of Sn–Zn lead-free solder alloys with radial heat flow and Bridgman-type apparatus.* Continuum Mechanics and Thermodynamics, 2012. **25**(6): p. 691-704.

258. Aksöz, S., & Maraşlı, N. , *Thermal and electrical conductivities of silver–indium–tin alloys.* Journal of Physics and Chemistry of Solids, 2012. **73**(7): p. 902-910.

259. Altıntas, Y., et al., *The measurements of electrical and thermal conductivity variations with temperature and phonon component of the thermal conductivity in Sn–Cd–Sb, Sn–In–Cu, Sn–Ag–Bi and Sn–Bi–Zn alloys.* International Journal of Thermal Sciences, 2016. **100**: p. 1-9.

260. Assael, M.J., et al., *Reference Correlations for the Thermal Conductivity of Liquid Bismuth, Cobalt, Germanium and Silicon.* J Phys Chem Ref Data, 2017. **46**(3).

261. Powell, R.W., & Tye, R. . *Experimental Determinations of the thermal and electrical conductivities of molten metals*. in *Thermodynamic and Transport Properties of Fluids* 1958.

262. Savchenko, I.V., S.V. Stankus, and A.S. Agadzhanov, *Investigation of thermal conductivity and thermal diffusivity of liquid bismuth within the temperature range of 545–970 K.* High Temperature, 2013. **51**(2): p. 281-283.

263. Aksöz, S., Maraşlı, N., Keşlioğlu, K., & Yıldız, F. , *Variations of thermal conductivity with temperature and composition of Zn in the Bi–[x]at.% Zn–2at.% Al alloys.* Thermochimica Acta, 2012. **547**: p. 1-5.

264. Aksöz, S., Ocak, Y., Maraşlı, N., & Keşlioğlu, K. , *Thermal conductivity and interfacial energy of solid Bi solution in the Bi–Al–Zn eutectic system.* Fluid Phase Equilibria, 2010. **293**(1): p. 32-41.

265. Saatci, B., Ari, M., Gündüz, M., Meydaneri, F., Bozoklu, M., & Durmuş, S. , *Thermal and electrical conductivities of Cd–Zn alloys.* Journal of Physics: Condensed Matter, 2006. **18**(47): p. 10643-10653.

266. Meydaneri, F., Saatccedil, B., & Ari, M. , *Thermo-electrical characterization of Lead-Cadmium (Pb-Cd) alloys.* International Journal of Physical Sciences 2012. **7**(48): p. 6210-6221.

267. Bilek, J., Atkinson, J., & Wakeham, W. , *Measurements of the Thermal Conductivity of Molten Lead Using a New Transient Hot-Wire Sensor.* International Journal of Thermophysics, 2007. **28**(2): p. 496-505.

268. I. V. Savchenko, S.V.S., and A. Sh. Agazhanov, *Measurement of the Thermal Conductivity and Diffusivity of Molten Lead in the interval 601–1000 K.* 2013. **115**: p. 83-87.

269. Aksöz, S., Ocak, Y., Maraşlı, N., & Keşlioğlu, K. , *Determination of thermal conductivity and interfacial energy of solid Zn solution in the Zn–Al–Bi eutectic system.* Experimental Thermal and Fluid Science, 2011. **35**(2): p. 395-404.

270. Duggin, M.J., *The thermal conductivities of aluminium and platinum.* Journal of Physics D: Applied Physics, 1970. **3**(5).

271. Brooks, R.F., Dinsdale, A. T., & Quested, P. N. , *The measurement of viscosity of alloys—a review of methods, data and models.* Measurement Science and Technology, 2005. **16**(2): p. 354-362.

272. Crawley, A.F., *The viscosities of some lead-antimony and lead-antimony-tin alloys.* Physics and Chemistry of Liquids, 2007. **2**(2): p. 77-85.

273. Mudry, S., Plevachuk, Y., Sklyarchuk, V., & Yakymovych, A. , *Viscosity of Bi–Zn liquid alloys.* Journal of Non-Crystalline Solids, 2008. **354**(35-39): p. 4415-4417.

274. Dobosz, A. and T. Gancarz, *Density, surface tension and viscosity of Ga-Sn eutectic based alloys with Zn additions.* Journal of Molecular Liquids, 2018. **264**: p. 600-606.

275. Rozhitsina, E.V., Gruner, S., Kaban, I., Hoyer, W., & Sidorov, V. E. , *Dynamic viscosities of pure tin and Sn-Ag, Sn-Cu, and Sn-Ag-Cu eutectic melts.* Russian Metallurgy (Metally), 2011. **2011**(2): p. 118-121.

276. Yakymovych, A., et al., *Viscosity and Electrical Conductivity of the Liquid Sn-3.8Ag-0.7Cu Alloy with Minor Co Admixtures.* J Mater Eng Perform, 2016. **25**(10): p. 4437-4443.

277. Sklyarchuk, V., Mudry, S., & Yakymovych, A. , *Viscosity of Bi-Ga liquid alloys.* Journal of Physics: Conference Series, 2008. **98**(6): p. 3.

278. Guanbao, M., Okhapkin, A. V., Konstantinova, N. Y., Sabirzyanov, A. A., & Pytsze, L. , *Kinematic viscosity of Mg-Al melts in the magnesium-rich portion.* Russian Metallurgy (Metally), 2013. **2013**(2): p. 90-95.

279. Sklyarchuk, V., Yakymovych, A., Shtablavyy, I., Shevernoha, I., Kozlovskii, M., Khairulin, R., & Stankus, S. , *Structure and physical properties of Pb–Sn melts.* Ukr. J. Phys, 2010. **55**(9): p. 980-987.

280. Birchenall, C.E., Harrison, A. J., & Balart, S. N. , *Determination of density changes during melting by X-ray absorption. .* Metallurgical Transactions A, 1980. **11**(7): p. 1213-1218.